AD-A182 512 EFFECT OF MOLECULAR WEIGHT OF ADDED POLYSTYRENE ON THE ORDER-DISORDER TRA..(U) CINCINNATI UNIV OH DEPT OF MATERIALS SCIENCE AND ENGINEERING.. S NOJIMA ET AL. 1/1

UNCLASSIFIED 01 JUL 87 TR-7 N00014-85-K-0245 F/G 11/9 NL

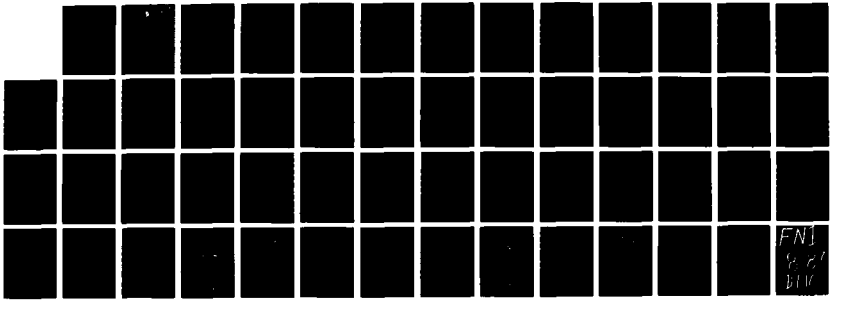

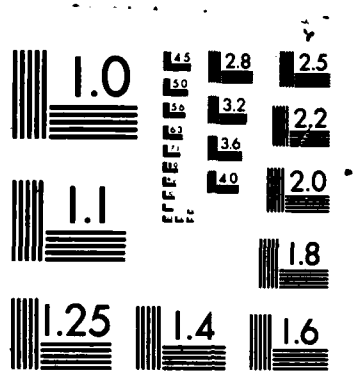

SECURITY CLASSIFICATION OF THIS PAGE

DTIC ELECTE JL 0 8 1987 D

REPORT DOCUMENTATION PAGE

DTIC FILE COPY

AD-A182 512

1b. RESTRICTIVE MARKINGS: None	
2b. DECLASSIFICATION/DOWNGRADING SCHEDULE	3. DISTRIBUTION/AVAILABILITY OF REPORT: Approved for Public Release, Distribution Unlimited
4. PERFORMING ORGANIZATION REPORT NUMBER(S): Technical Report No. 7	5. MONITORING ORGANIZATION REPORT NUMBER(S)
6a. NAME OF PERFORMING ORGANIZATION: University of Cincinnati; 6b. OFFICE SYMBOL (If applicable)	7a. NAME OF MONITORING ORGANIZATION: ONR
6c. ADDRESS (City, State, and ZIP Code): Clifton Avenue, Cincinnati, OH 45221	7b. ADDRESS (City, State, and ZIP Code): 800 North Quincy Avenue, Arlington, VA 22217
8a. NAME OF FUNDING/SPONSORING ORGANIZATION: ONR; 8b. OFFICE SYMBOL (If applicable)	9 PROCUREMENT INSTRUMENT IDENTIFICATION NUMBER: N-00014-85-K-0265
8c. ADDRESS (City, State, and ZIP Code): 800 North Quincy Avenue, Arlington, VA 22217	10. SOURCE OF FUNDING NUMBERS: PROGRAM ELEMENT NO.; PROJECT NO.; TASK NO.: NR 356-655; WORK UNIT ACCESSION NO

11 TITLE (Include Security Classification)
Effect of Molecular Weight of Added Polystyrene on the Order-Disorder Transition of Styrene-Butadiene Diblock Copolymer

12 PERSONAL AUTHOR(S)
S. Nojima and R. J. Roe

13a TYPE OF REPORT	13b TIME COVERED FROM ____ TO ____	14. DATE OF REPORT (Year, Month, Day)	15 PAGE COUNT
Technical		July 1, 1987	51

16. SUPPLEMENTARY NOTATION
Accepted for Publication in Macromolecules

17 COSATI CODES		
FIELD	GROUP	SUB-GROUP

18. SUBJECT TERMS (Continue on reverse if necessary and identify by block number)
Block Copolymer, Order-Disorder Transition, Miscibility, Polystyrene, Styrene-Butadiene Block Copolymer, Small-Angle X-ray Scattering

19 ABSTRACT (Continue on reverse if necessary and identify by block number)

The change in the order-disorder transition temperature of block copolymer, induced by the addition of homopolymer, is investigated. Analysis of the theoretical expression based on the random phase approximation shows that the direction of the change in the transition temperature is determined by the length of the added homopolymer in relation to the length of the block copolymer and the overall composition of the monomers in the mixture. Small-angle X-ray scattering measurements are performed with mixtures containing a styrene-butadiene diblock copolymer and a polystyrene of various molecular weight. The observed shape of the scattered intensity curve, the angular position of the peak intensity, and the spinodal temperature for the micro-phase separation all agree well with the prediction from the theory. The values of the interaction energy density Λ determined from the results agree fairly well with values determined previously from cloud point data. A

20 DISTRIBUTION/AVAILABILITY OF ABSTRACT	21 ABSTRACT SECURITY CLASSIFICATION
☒ UNCLASSIFIED/UNLIMITED ☐ SAME AS RPT ☐ DTIC USERS	
22a NAME OF RESPONSIBLE INDIVIDUAL: Dr. Kenneth J. Wynne	22b TELEPHONE (Include Area Code): 202-696-4409; 22c OFFICE SYMBOL

DD FORM 1473, 84 MAR 83 APR edition may be used until exhausted. All other editions are obsolete.

87 SECURITY CLASSIFICATION OF THIS PAGE

Abstract (cont'd.)

strong scattering increasing in intensity with decreasing scattering angle is observed with some of the samples at temperatures near or below the transition temperature. This is not predicted by the theory but could be explained in terms of the possible presence of a transition region in the phase diagram in which ordered and disordered phases of differing compositions coexist.

OFFICE OF NAVAL RESEARCH

Contract N00014-85-K-0245

Task No. 356-655

TECHNICAL REPORT NO. 7

Effect of Molecular Weight of Added Polystyrene on the Order-Disorder Transition of Styrene-Butadiene Diblock Copolymer

by

S. Nojima and R. J. Roe

Accepted for Publication in
Macromolecules

Department of Materials Science
and Engineering
University of Cincinnati
Cincinnati, Ohio 45221-0012

July 1, 1987

I. Introduction

Blends of block copolymer AB and homopolymer A exhibit a variety of phase transition and separation behavior that depends on the temperature, the concentration of the added homopolymer, and the compositional structure of the block copolymer molecule. At lower temperatures, microphase separation of blocks in the copolymer results in the formation of a mesophase in which the microdomains are ordered on a macrolattice. With increase in temperature such an ordered phase may be transformed into a disordered phase in which blocks A and B are intimately mixed. In both the ordered and disordered phases of the block copolymer the added homopolymer may, however, be only partially miscible, giving rise to the coexistence of two demixed phases. The interaction of such macrophase separation with the order-disorder transition produces a fascinating complexity in the resulting phase diagram.

We previously investigated[1,2] blends of styrene-butadiene diblock copolymer with polystyrene or polybutadiene by means of small-angle X-ray scattering and light scattering techniques, and constructed phase diagrams by combining results of these observations with the principles of thermodynamics governing phase relations. In the present study we explore one particular region of the phase diagram in greater detail. We focus our attention on the change in the order-disorder transition temperature induced by the addition of homopolymer of various molecular weight. We then compare our experimental results with predictions based on the theoretical model employing the random phase approximation.[3,4]

As has been stressed by deGennes,[5] properties of amorphous mixtures involving only polymeric components can be described adequately by means of mean-field theories. Thus the Flory-Huggins free energy of mixing serves well as the basis for discussion of polymer blends containing homopolymers and random copolymers, if the dependence on temperature and composition of the interaction parameter is properly taken into account. The method of random phase approximation applied to amorphous polymer blends leads to an expression for the structure factor $S(q)$ as a function of the wave vector, $q = 4\pi\sin\theta/\lambda$. This is also a mean-field theory, and its expression for $q = 0$ reduces exactly to the second derivative of the Flory-Huggins free energy of mixing. The same expression for $S(q)$ was also derived recently by two other methods[6,7] which are very different in formalism but nevertheless share the mean-field nature. The expression can be regarded as an extension of the Flory-Huggins treatment to blends containing block copolymers in disordered state. Its usefulness has previously been demonstrated in reference to observations[8-10] made with pure block copolymers. One of the objectives of the present study is to ascertain its validity in detail by comparing it against observations obtained with blends containing a block copolymer and a homopolymer.

II. Predictions from Random Phase Approximation Theory

A. Explicit expression for $S(q)$.

When the method of random phase approximation is applied to polymer systems containing any number of polymeric components but

consisting as a whole of only two monomeric species 1 and 2, one obtains the expression[4] for the structure factor S(q), or the Fourier transform of the density correlation function, as

$$1/S(q) = Q(q) - 2\Lambda/kT \tag{1}$$

with

$$Q(q) = \frac{S_{11}(q) + S_{22}(q) + 2S_{12}(q)}{S_{11}(q)S_{22}(q) - S_{12}^2(q)} \tag{2}$$

where $S_{ij}(q)$ is the Fourier transform of the correlation function between species i and j in the hypothetical case where there is no interaction between different molecules, each polymer molecule thus behaving "ideally." In equation (1), Λ is the interaction energy density[11,12] between the species, which is related to the usual χ parameter by

$$\Lambda = \chi RT/V_u \tag{3}$$

where V_u is some reference volume which is assumed, often implicitly, as the basis of definition of χ. [Note also that S(q) and $S_{ij}(q)$ in equations (1) and (2) have a dimension of volume, in contrast to the customary practice of defining S(q) dimensionless.]

The system under consideration consists of a mixture of homopolymer A having molecular volume V_h and diblock copolymer AB having molecular volumes V_1 and V_2 for the blocks A and B, respectively. The volume fraction of the homopolymer in the mixture is equal to ϕ_h. The composition of the block copolymer is represented by the volume fractions f_1 and f_2 of the two types

of species in the molecule, i.e., $f_1 = V_1/(V_1 + V_2)$ and $f_2 = V_2/(V_1 + V_2)$. For $S_{ij}(q)$'s we then have

$$S_{11}(q) = (1-\phi_h)V_1 f_1 g(x_1) + \phi_h V_h g(x_h) \quad (4)$$

$$S_{22}(q) = (1-\phi_h)V_2 f_2 g(x_2) \quad (5)$$

$$S_{12}(q) = (1-\phi_h)(V_1+V_2)(f_1/x_1)(f_2/x_2)[1-\exp(-x_1)][(1-\exp(-x_2)] \quad (6)$$

The function g(x) is the Debye correlation function for a gaussian chain

$$g(x) = 2(x+e^{-x}-1)/x^2 \quad (7)$$

with the variable x_1, x_2 and x_h defined by

$$x_1 = q^2R_1^2/6; \quad x_2 = q^2R_2^2/6; \quad x_h = q^2R_h^2/6 \quad (8)$$

where R_1, R_2 and R_h are the rms end-to-end distances of block A and block B in the copolymer and of the homopolymer, respectively. In writing equations (1)-(6) we have followed the spirit enunciated in an earlier publication,[13] namely, our preference of expressing the configurational properties of a polymer chain in terms of the molecular volume V and the end-to-end distance R rather than in terms of the number of segments N and the segment size a. This is especially desirable when the differences in the monomer size and the chain flexibility between the two species A and B are to be expressly incorporated in the equations. As a result these equations, and equation (6) in particular, are slightly modified from those originally given by Leibler.[4,14]

B. Variation in spinodal temperature T_s.

The spinodal temperature T_s is obtained from equation (1) as the temperature at which $S(q^*)$ diverges, where q^* is the value of q rendering Q(q) minimum. We are interested in defining the conditions under which T_s either increases or decreases as a homopolymer is added to a block copolymer. For this purpose we obtain numerical solution of equation (1) as a function of two variables: V_h/V_c (where $V_c = V_1 + V_2$), expressing the relative size of the homopolymer to that of the copolymer, and f_1, expressing the relative size of the block A in the copolymer. The results are given in Figures 1 to 3 in terms of $kT_s/\Lambda V_c$ (which is equivalent to $1/N\chi_s$ in Leibler's notation[4]) against ϕ_h. (In this numerical calculation the flexibilities of the two types of chains are assumed equal, i.e., $V_1/R_1^2 = V_2/R_2^2$.) They show that addition of small homopolymer molecules depresses T_s, while addition of large homopolymer molecules raises T_s. The molecular volume ratio V_h/V_c which is at the crossover from depression to elevation of T_s depends on the composition f_1 of the block copolymer, as is shown in Figure 4. For a symmetrical block copolymer ($f_1 = 0.5$), this crossover occurs when the size of the homopolymer is almost exactly equal to a quarter of the size of the copolymer. This is in agreement with the results obtained by Whitmore and Noolandi[15] by a somewhat different approach. It is interesting to note that the same result was also obtained earlier by Krause[16] by a much more macroscopic consideration. The results in Figures 1-4 can be summarized qualitatively as follows: the spinodal temperature T_s is raised on the addition

of homopolymer A if: (i) the chain length of the homopolymer is large and (ii) its addition makes the overall composition of A and B in the mixture more symmetrical. The first of these two factors can be easily rationalized in terms of the smaller entropy of mixing offered by large homopolymer molecules. The second can be understood in analogy with the fact that, in a binary mixture of homopolymers A and B (with Λ positive), demixing occurs at higher temperatures if the composition is more symmetrical, and also with the fact[4] that among pure block copolymers having the same total length the order-disorder temperature is higher for a more symmetrical copolymer.

C. Microphase separation vs. macrophase separation.

Next we investigate how the value of q*, at which Q(q) becomes minimum, varies with addition of homopolymer. In Figure 5, the values of q^*R_c (where R_c is the end-to-end distance of the copolymer molecule) are plotted against the volume fraction ϕ_h of the homopolymer. (In this calculation, the copolymer is assumed symmetrical, that is, f_1 is equal to 0.5 and the two block chains have equal flexibility: $V_1/{R_1}^2 = V_2/{R_2}^2$.) It is seen that q* always decreases with addition of homopolymer, and the rate of decrease is larger with a larger homopolymer. The value of q* denotes the predominant size scale of the structure that emerges at T_s when S(q*) diverges. These mixtures showing $q^* \neq 0$ will eventually undergo <u>micro</u>phase separation on lowering the temperature. It is possible, by addition of a sufficient amount of homopolymer, to reduce q* eventually to zero. Such a mixture would then undergo a <u>macro</u>phase separation

on lowering the temperature. Thus, one can induce a transition from a microphase separation to a macrophase separation behavior by addition of an increasing amount of homopolymer. The nature of this changeover from the microphase separation to macrophase separation behavior can be understood more clearly with reference to Figures 6 and 7. Here S(q) when $T \to \infty$ (i.e., when the term $2\Lambda/kT$ is equal to zero) is plotted against q for a number of different mixtures. To facilitate later comparison with our experimental results, these curves are calculated with parameter values appropriate for the blends containing polystyrene (M_w = 35,000 in Figure 6 and M_w = 70,000 in Figure 7) added to a styrene-butadiene diblock copolymer (M_w of copolymer 22,000, weight fraction of styrene 76.6%). The maximum in these plots for S(q) against q gives the value of q*. In Figure 6, calculated for the added polystyrene of M_w 35,000, each curve has a single maximum, and the value of q* decreases continuously with increasing homopolymer fraction until it reaches zero at ϕ_h between 0.55 and 0.60. Thereafter, q* remains at zero. In Figure 7, calculated for the added polystyrene of M_w 70,000, some of the curves have two maxima, one at $q \neq 0$ and another at $q = 0$. Of these two, the absolute maximum, which grows first to infinity on lowering the temperature, gives q*. Thus, with increasing fraction of added polystyrene, q* makes a discontinuous jump from some finite value to zero. A blend with a finite value of q* undergoes a <u>micro</u>phase separation on cooling, while a blend with q* = 0 undergoes a <u>macro</u>phase separation just as a mixture of two homopolymers does. Figures 6 and 7 thus show that, on addition

of homopolymers, the changeover from microphase separation to macrophase separation behavior can occur either gradually or abruptly, depending on the molecular weight of the homopolymer added. Figure 8 plots the change in q* induced with increasing amount of polystyrene of various molecular weight added to the styrene-butadiene diblock copolymer. It clearly illustrates the point discussed above, that is, that with lower molecular weight polystyrene q* approaches continuously toward zero, while with higher molecular weight polystyrene the value of q* falls discontinuously to zero.

D. Phase relations.

The knowledge of the structure factor S(q) allows us to predict the spinodal temperature as a function of the composition of the blends, but not the phase diagram itself. To construct the phase diagram, depicting the regions of stable phases and the compositions of coexisting phases, one requires the expression for the free energy, of which S(q) is only the second order term. No general theory is yet available that gives the free energy for the mixture of homopolymer and block copolymer. (Noolandi and his coworkers[15,17] give the free energy for the special case of lamellar morphology.) Useful inference on the various trend in the phase diagram, however, can be obtained from the knowledge of the spinodal temperature. In Figure 9 we therefore plot the spinodal temperatures calculated as a function of composition for the mixtures containing the styrene-butadiene diblock copolymer mentioned above and either polystyrene of M_w 70,000 or polystyrene of M_w 35,000. The spinodal was calculated from

equation (1) by using the following value of Λ, which is the average of nine determinations based on the cloud point curves of mixtures of polystyrene and polybutadiene or their random copolymer[12]

$$\Lambda = 0.718 \pm 0.051 - (0.0021 \pm 0.00045)(t-150^{\circ}C) \quad (cal/cm^3) \qquad (9)$$

In Figure 9, the thick curves give the spinodal temperatures for microphase separation ($q^* \neq 0$) and the thin curves the spinodal temperatures for macrophase separation ($q^* = 0$). For the latter, the condition for spinodal can be obtained from equation (1) by requiring that $1/S(0) \to 0$, i.e.,

$$0 = \frac{1}{\phi_h V_h} + \frac{1}{(1-\phi_h)(V_1+V_2)} - \frac{2\Lambda}{kT} f_2^2 \qquad (10)$$

Equation (10) is identical to the condition for spinodal obtainable from the Flory-Huggins free energy of mixing a homopolymer and a copolymer with an effective interaction energy density equal to Λf_2^2. The upper diagram in Figure 9, calculated for the mixture containing polystyrene of M_w 70,000, shows that the two curves for microphase separation and macrophase separation meet at an angle at a composition to the left of the critical point of the macrophase separation. In contrast, the lower diagram in Figure 9, calculated for the mixture containing polystyrene of M_w 35,000, shows that the curves for microphase separation and macrophase separation meet with a common tangent, and that this mixture does not exhibit a critical point. The differences between these two types of diagrams are reflected

also in Figure 8, where the change in q* from a finite, non-zero value to zero occurs discontinuously in the case of the mixture containing polystyrene of M_w 70,000, whereas the change occurs continuously in the case of the mixture containing polystyrene of M_w 35,000.

III. Experimental Section

A. Materials.

The styrene-butadiene diblock copolymer is the one designated as copolymer 75/25 in our earlier study,[18] and contains 76.6% by weight of styrene. It was kindly synthesized by Dr. H. L. Hsieh of Philips Petroleum Company, who provided us with the characterization data: M_n = 21,000 (by GPC), M_w/M_n = 1.05 (by GPC), 48% trans 1,4 and 24% cis 1,4. The styrene content was determined in this laboratory by NMR. An independent characterization of this polymer was also given by Krause et al.[19] The polystyrene samples of various molecular weights were purchased from the Pressure Chemical Company, and all of them are said to have M_w/M_n ratio equal to or less than 1.05.

Compositions of all the mixture samples prepared for study are summarized in Table I. Of these, the ones containing polystyrene of M_w 100,000 were turbid. The remaining 13 samples were all visually clear at room temperature and were examined further by means of small-angle X-ray scattering at various temperatures. Samples for these measurements, except the one containing polystyrene of M_w 50,000, were prepared by mixing the

block copolymer and polystyrene (without solvent) mechanically under vacuum at temperatures somewhat above 200°C. The mixtures containing polystyrene of M_w 50,000 were prepared by first dissolving the two polymers in benzene and then evaporating the solvent. To destroy the effect of casting conditions, the samples were heated well into the disordered region and cooled before any X-ray scattering measurements were taken.

B. Method of measurement.

All scattering curves were obtained with a Kratky camera fitted with a one-dimensional position-sensitive detector made by M. Braun Company. Nickel-filtered CuKα radiation supplied by a Philips XRG 3100 generator operating at 45 kV and 35 mA was used throughout. The procedure of measurements was essentially similar to that described earlier.[1,18] Background scattering correction was made by subtracting the scatterings from pure polystyrene and pure polybutadiene, each weighted according to the amounts of styrene and butadiene present in the sample. The correction for the slit-length smearing was applied by means of Strobl's algorithm.[20]

C. Data analysis.

To convert from weight into volume of the polymers, the following specific volumes were used. For polystyrene[21]

$$v_{sp} = 0.9217 + 5.412\times10^{-4}t + 1.687\times10^{7}t^{2} \quad \text{(above } T_g\text{)} \qquad (11)$$

and for polybutadiene[18]

$$v_{sp} = 1.1138 + 8.24\times10^{-4}t \qquad (12)$$

These specific volumes are also used for the calculation of electron density differences at various temperatures. The rms end-to-end distance, required for comparison with theoretical predictions from equation (1), was estimated from $R = AM^{1/2}$, where A equals 0.0674 $nm.mole^{1/2}/g^{1/2}$ for polystyrene[22] and 0.09 for polybutadiene.[23]

IV. Results

A. Scattering curves.

The intensity data obtained with five of these samples are shown in Figures 10-14 which are all plotted on the same scale to facilitate comparison. In these plots the abscissa is the scattering angle $s = q/2\pi = 2\sin\theta/\lambda$ and the ordinate gives $S(q) = I(s)/(\Delta\rho)^2$ where I(s) is the scattered intensity (after correction for slit-length smearing) in absolute unit ($electron^2/nm^3$) and $\Delta\rho$ is the difference in electron density ($electron/nm^3$) between polystyrene and polybutadiene.

In all cases shown in Figures 10-14 the scattered intensity increases steadily as the temperature is lowered. We estimate, as will be described later, that the formation of mesophase, induced by microphase separation, begins very approximately at 130, 150 and 200°C for the mixtures shown in Figures 10, 11 and 12, respectively. The data shown in Figures 13 and 14 all correspond to temperatures below the microphase separation temperature. The peak intensity I(s*) shows a gradual variation over a temperature range exceeding 100°, and no discontinuity is present to indicate the onset of mesophase formation. Such a

continuous change in I(s*) with temperature was previously observed[8] even with pure block copolymers. Evidently, the process of mesophase formation is unlike the formation of crystalline solid which involves nucleation and growth of highly ordered structure even at temperatures only moderately below the melting point.

Figure 14 shows that the scattered intensity curves there consist of two components, one having the peak at a finite s, and another increasing in intensity rapidly as $s \to 0$, suggesting that its peak is probably located at $s = 0$. The contribution by the second component in varying degrees can be noticed in Figures 10-13 as well, its magnitude apparently increasing with increasing molecular weight of polystyrene. The presence of such a component having the peak at $s = 0$ is not predicted by the theory. For example, in Figures 10 and 11 the solid curves drawn were calculated by means of equations (1) and (2). In calculating these curves, the value of the λ parameter was adjusted to obtain a match in the calculated and observed peak intensity, but otherwise no adjustable parameters were involved. Three observations can be made. (1) The angle of maximum intensity, s* or q*, shows generally good agreement between the observed and calculated intensity curves. (2) The degree of fit is about the same, irrespective of whether the temperature is above or moderately below the microphase separation temperature. (3) The observed scattered intensity at angles smaller than s* is much enhanced in comparison to the calculated one, evidently due to the contribution by the component of scattering with peak at

$s = 0$. The possible reason for the presence of the latter component is discussed later in the Discussion section.

B. Peak angle q^*.

Figure 15 plots the variation in the peak angle s^* with the volume fraction of polystyrene of M_w 2,200 and of M_w 17,500. Figure 16 similarly plots the variation in s^* with the molecular weight of polystyrene when the volume fraction of the latter is held at 40% or 60%. (The values of s^* were evaluated from the observed intensity curves by the curve fitting method, described in the next section, which allows for the presence of two independent components of scattering with maxima at $s^* = 0$ and $s^* \neq 0$.) In Figures 15 and 16, the solid curves show the s^* values at which $Q(q)$, given by equations (2), (4)-(6), becomes minimum. This is an absolute comparison involving no adjustable parameters, and the agreement between the observed and calculated values is very good.

With all the mixtures the s^* value remains independent of temperature, except that there is a tendency for the value to decrease slightly as the temperature is lowered much below the microphase separation temperature (although such a tendency may not be readily discernable on visual inspection of Figures 10-14). Earlier, Bates and Hartney[10] reported an apparently similar shift in the peak angle q^* with temperature, in their SANS data on diblock copolymer of 1,4-polybutadiene and 1,2-polybutadiene. But their observation, made <u>above</u> the microphase separation temperature, may not be related to our result.

C. Correlation length ξ.

Following the suggestion by de la Cruz and Sanchez[7] one can expand Q(q) around q* to the second order and obtain an approximation to equation (1) in the Ornstein-Zernike form

$$S(q) = S(q^*)/[1+\xi^2(q-q^*)^2] \qquad (13)$$

where ξ is the correlation length associated with the decay of short range order and is given by

$$\xi^2 = 1/4Q''(q^*)/(\Lambda_s/kT_s - \Lambda/kT) \qquad (14)$$

T_s being the spinodal temperature and Λ_s the value of Λ at T_s. Equation (13) suggests that a plot of $[S(q^*)/S(q)-1]^{1/2}$ against q/q^* will produce a straight line of slope ξq^*. This is demonstrated in Figure 17 for the data obtained with the sample containing 60% polystyrene of M_w 2,200. The good straight lines obtained show that equation (1) is capable of representing the shape of the scattered intensity curve around the peak faithfully. In Figure 18 the values of ξ thus evaluated for all the samples containing polystyrene of M_w 2,200 are plotted against temperature. From these values of ξ, the spinodal temperature and the value of the interaction energy density Λ at various temperatures can be obtained, as described shortly below. For mixtures containing polystyrene of higher molecular weight the above method of determining ξ becomes impractical because of the presence of the extraneous component of scattering with a peak at q* = 0, as shown in Figures 12-14. Such curves were fitted to the following empirical equation,

$$S(q) = \frac{S_1(0)}{1 + \xi_1^2 q^2} + \frac{S_2(q^*)}{1 + \xi_2^2 (q-q^*)^2} \qquad (15)$$

which assumes two independent contributions to the total scattered intensity, the first arising from the long-range concentration fluctuation according to the Ornstein-Zernike form and the second arising from the short-range fluctuation according to equation (13). The best fit to the observed curves were determined by adjusting the five parameters $S_1(0)$, ξ_1, q^*, $S_2(q^*)$ and ξ_2. An example of such a fit is given in Figure 19. The estimation of the best values of the parameters q^*, $S_2(q^*)$ and ξ_2 was relatively easy and their values were not much affected even when a fairly wide latitude was given to the choice of values of $S_1(0)$ and ξ_1. Among the values of q^*, $S(q^*)$ and ξ reported or incorporated into further analysis in this paper, those pertaining to mixtures containing 60% polystyrene of M_w 10,300 and all concentrations of polystyrene at higher molecular weight were obtained by this curve fitting method. In contrast to this, meaningful values of the two parameters $S_1(0)$ and ξ_1 defining the first term in equation (16) were difficult to obtain and therefore no attempt has been made to interpret them quantitatively.

D. Spinodal temperature T_s.

The spinodal temperature T_s for microphase separation can be determined by two independent methods, one from the plot of $1/S(q^*)$ against $1/T$ and the other from the plot of ξ^{-2} against $1/T$. The first method relies on the variation of the scattered intensity with temperature, and requires the intensity measured

in absolute scale. The second method relies on the variation with temperature of the shape of the scattered intensity curve around q^*, and does not require the intensity to be expressed in absolute unit. An example of the plot in accordance with the second method is given in Figure 20. In the case of the first method, we note that, by assuming $\Lambda = A + BT$, one can write from equation (1)

$$1/S(q^*) = Q(q^*) - 2B/k - 2A/kT \qquad (16)$$

This means that the plot of $1/S(q^*)$ against $1/T$ should have the same slope, $-2A/k$, with all blends involving homopolymers and copolymers which contain only styrene and butadiene monomeric units. With suitable shifts along the $1/T$ axis, all these plots should be superposable into a single curve. This, indeed, is achieved in Figure 21 where data obtained with mixtures containing polystyrene of M_w 2,200 are shown and also in Figure 22 where data obtained with mixtures containing 60% of polystyrenes of various molecular weights are shown. The straight line drawn in both figures corresponds to $A = 1.19$ cal/cm^3. The spinodal temperature can be obtained from the extent of shift along the $1/T$ axis for the individual data. The value of T_s determined by these two methods are listed in Table II. The temperature of actual onset of mesophase formation is expected[4] to be somewhat higher than T_s, and appears to be, in general, about 20° above T_s as estimated from the point of deviation of the observed $S(q^*)$ from the straight line in Figures 20 to 22.

In Figures 23 and 24 the T_s values determined from $S(q^*)$ and from ξ are compared. The agreement between these two sets of data is excellent. Also drawn are the curves showing the values of T_s calculated from equation (1) with the Λ values given by equation (9). The agreement between the curves and those T_s values determined directly from the experimental data is, although not as good, still fairly satisfactory, and demonstrates that equation (1) can be utilized to predict T_s with some degree of confidence when the values of Λ are obtained by some other independent method.

E. Interaction energy density Λ.

Another method of testing the validity of equation (1), which is complementary to that depicted in Figures 23 and 24, is to evaluate the values of the interaction energy density Λ from the experimental data and compare them with equation (9). There are two independent methods of determining Λ values, one based on $I(q^*)$ and another based on ξ, each corresponding to one of the two methods of determining T_s mentioned above. In the first method, we rewrite equation (1) as

$$2\chi/kT = Q(q^*) - 1/S(q^*) \qquad (17)$$

and substitute observed values of $I(q^*)/\Delta\rho^2$ for $S(q^*)$ and then calculate $Q(q^*)$ by means of equations (2), (4)-(7) which involve molecular volumes and end-to-end distances of copolymer blocks and homopolymer. Figure 25 gives the Λ values thus evaluated, and the broken straight line represents the average of these evaluated Λ values that is forced to go through $\Lambda = 1.19$ cal/cm^3

at T = 0K, to conform to the common slope in the plots given in Figures 21 and 22. This gives

$$\Lambda = 1.19 - 5.0\times10^{-4}T$$

$$= 0.98 - 5.0\times10^{-4}(t^{\circ}C-150^{\circ}C) \qquad (18)$$

The solid straight line in Figure 25 represents equation (9), which was previously determined from the cloud points of blends of polystyrene and polybutadiene or their copolymers. The second method of evaluating Λ values relies on

$$\Lambda/kT = 1/2Q(q^*) - 1/4Q''(q^*)/\xi^2 \qquad (19)$$

where ξ is given the experimentally determined values and $Q(q^*)$ and $Q''(q^*)$ are calculated from the knowledge of the molecular volumes and end-to-end distances by means of the theoretical expressions. Figure 26 gives the Λ values thus determined, which are generally lower than those given in Figure 25 and are thus in better agreement with the solid line representing equation (9). Of the two independent methods represented by Figures 25 and 26, the first one based on the peak intensity $I(q^*)$ gives a slightly better precision, but is subject to the error in the scaling of the observed relative intensity into absolute intensity scale. Examination of Figures 25 and 26 suggests that there is a discernable trend in the Λ values that depends on molecular weight and composition, and the overall spread of the data points there is due partly to these effects.

IV. Discussion

Most of the qualitative and semi-quantitative features predicted by the theory,[4] embodied in equations (1)-(9), are confirmed by the experimental observations. These include the fact (1) that the microphase separation temperature is lowered by the addition of polystyrene, (2) that the magnitude of the depression is larger with larger amounts of lower molecular weight polystyrene, (3) that the peak intensity angle q* agrees almost quantitatively with the theoretical prediction, (4) that the shape of the scattered intensity curve around the peak is well reproduced by the theory, (5) that the spinodal temperatures T_s for microphase separation that are evaluated by two independent methods, one based on the peak intensity I(s*) and the other based on the correlation length ξ, agree well with each other, and (6) that the values of the interaction energy density Λ, evaluated on the basis of I(s*) and ξ separately, agree approximately with the values determined previously from the study of macrophase separation of homopolymers and random copolymers.

The only feature that has not been explained so far in terms of the theory is the component of scattering which increases in intensity rapidly as $q \to 0$ and is observed with many of the blends. This low angle component of scattering becomes more pronounced with increasing molecular weight of polystyrene, as the series of data shown in Figures 10-14 illustrate. Consultation of Table II, however, reveals that most of the data exhibiting a significant low-angle component are obtained at

temperatures near or below the spinodal temperature. The low-angle component thus appears to be associated with the formation of mesophase, and this is unlikely to be explained solely on the basis of the theory which applies to the disordered phase.

With pure block copolymer the order-disorder transition is predicted to be of first order according to Leibler's theory.[4] When a mixture of block copolymer with homopolymer is cooled toward its T_s, however, the formation of mesophase is expected to occur over a range of temperature and not at a single transition temperature. This follows from the thermodynamic requirement[24] that, in the phase diagram of a system of binary components, two different single phase regions are always separated by a region of two coexisting phases, if the underlying transition is of first order. Figure 9 gives the diagrams, predicted from the theory, showing the spinodal temperature against the composition of the mixture. To explain the phase relations observed experimentally, however, we need a phase diagram giving binodals rather than spinodals. There is, at present, no theory which allows us to predict binodals quantitatively. Instead, we may construct a phase diagram having qualitative validity from speculative considerations based on Figure 9 and the thermodynamic principles. Such an attempt is illustrated in Figure 27, where phase diagrams a, b and c correspond to cases where the molecular weight of added homopolymer is successively smaller while the block copolymer remains the same. Some of the features here are modeled after the experimentally determined

phase diagrams obtained in our previous study.[2] Here L and M denote disordered and ordered phases, respectively. In the region denoted by L_1+L_2, two disordered phases coexist. Its binodal should be describable by the Flory-Huggins free energy of mixing, and the highest temperature on this binodal, being the critical point, should coincide with the highest temperature of the spinodal curve in Figure 9. In diagram c, region M_1+M_2 arises instead of region L_1+L_2, and denotes the condition for the coexistence of two mesophases of different compositions. The presence of a M_1+M_2 region has not yet been demonstrated experimentally. In all three diagrams, the line AC denotes a eutectic temperature at which three phases, A, B and C, coexist. Our chief concern here is the region denoted M+L above the eutectic temperature. The upper binodal of this M+L region should lie somewhat above the spinodal line for microphase separation given in Figure 9. Let us study what will happen when we start with a mixture having a composition denoted by an arrow in the disordered, homogeneous state, and cool it. In the case of diagram a it will hit the binodal of L_1+L_2 region and separate into two disordered phases having very different compositions. The mixture will then turn cloudy. In the case of diagrams b and c it will, on cooling, first encounter the upper binodal of M+L region, at which a mesophase, having a composition corresponding to the lower binodal at the temperature, starts to appear. Thermodynamically it is a macrophase separation, and as the temperature is gradually lowered, the volume of mesophase increases and the compositions of the disordered phase and the

mesophase both shift along the upper and lower binodals, respectively. Visually observable turbidity might not develop, however, because the composition difference between the disordered phase and the emerging mesophase is relatively small and, moreover, the particle size of the latter might not grow large for kinetic reasons. The presence of such coexisting phases of small sizes nevertheless might produce sufficient scattering of X-rays observable at very small angles. The validity of the above explanation can only be confirmed fully by quantitative comparison of our data with any theories capable of predicting binodals that might be developed in the future. The speculative discussion offered above, however, seems to be able, for the moment, to explain most of the qualitative features observed in our study.

Acknowledgment

This work was supported, in part, by the Office of Naval Research. We gratefully acknowledge stimulating discussions with Dr. L. Leibler.

References

1. Zin, W.-C. and Roe, R. J., Macromolecules 1984, 17, 183.

2. Roe, R. J. and Zin, W.-C., Macromolecules 1984, 17, 189.

3. deGennes, P.-G., J. Phys. (Paris) 1970, 31, 235.

4. Leibler, L., Macromolecules 1980, 13, 1602.

5. deGennes, P.-G., "Scaling Concepts in Polymer Physics," Cornell University Press, Ithaca, NY, 1979.

6. Benoit, H. and Benmouna, M., Macromolecules 1984, 17, 535; Benoit, H., Wu. W., Benmouna, M., Mozer, B., Bauer, B., and Lapp, A., Macromolecules 1985, 18, 986.

7. de la Cruz, M. O. and Sanchez, I. C., Macromolecules 1986, 19, 2501.

8. Roe, R. J., Fishkis, M., and Chang, J. C., Macromolecules 1981, 14, 1091.

9. Mori, K., Hasegawa, H., and Hashimoto, T., Polymer J. 1985, 17, 799.

10. Bates, F. S. and Hartney, M. A., Macromolecules 1985, 18, 2478.

11. Roe, R. J., Adv. Chem. Ser. 1979, 176, 599.

12. Roe, R. J. and Zin, W.-C., Macromolecules 1980, 13, 1221.

13. Roe, R. J., Macromolecules 1986, 19, 728.

14. Leibler, L. and Benoit, H., Polymer 1981, 22, 195.

15. Whitmore, M. D. and Noolandi, J., Macromolecules 1985, 18, 2486.

16. Krause, S., in "Colloidal and Morphological Behavior of Block and Graft Copolymers," G. E. Molau, ed., Plenum, NY, 1971, p. 223; Krause, S., Macromolecules 1970, 3, 84.

17. Hong, K. M. and Noolandi, J., Macromolecules 1983, 16, 1083.

18. Rigby, D. and Roe, R. J., Macromolecules 1986, 19, 721.

19. Krause, S., Lu, Z. H., and Iskandar, M., Macromolecules 1982, 15, 1076.

20. Strobl, G. R., Acta Crystallogr., 1970, A26, 367.

21. Richardson, M. J. and Savill, N. G., Polymer 1977, 18, 3.

22. Tangari, C., King, J. S., and Summerfield, G. C., Macromolecules 1982, 15, 132.

23. Brandrup, J. and Immergut, E. H., Eds., "Polymer Handbook," Second Edition, Wiley, NY, 1975, Section V.

24. Gordon, P., "Principles of Phase Diagrams in Materials Systems," McGraw-Hill, NY, 1968.

Legend to Figures

Figure 1. The calculated spinodal temperature T_s of microphase separation is plotted against the volume fraction ϕ_h of homopolymer in the blend. The block copolymer has A and B blocks of equal length. The ratio of the molecular volume V_h of homopolymer A to the molecular volume V_c of the copolymer is indicated for each curve. The ordinate $kT_s/\Lambda V_c$, where Λ is the interaction energy density, is identical to $1/\chi N$ in the usual notation.

Figure 2. Similar to Figure 1, but for the case where the volume fraction f_1 of block A in the diblock copolymer is equal to 0.65.

Figure 3. Similar to Figure 1, but for the case where the volume fraction f_1 of block A in the diblock copolymer is equal to 0.30.

Figure 4. The ordinate gives the molecular volume V_h of homopolymer A (in relation to the molecular volume V_c of the copolymer) which, when added to the copolymer, neither depresses nor elevates the spinodal temperature T_s for microphase separation (in the limit of $\phi_h \to 0$). The abscissa gives the volume fraction f_1 of block A in the copolymer.

Figure 5. The calculated change in the peak scattering angle q* is plotted against the volume fraction ϕ_h of added homopolymer A, for the various ratios of V_h/V_c indicated. The volume fraction f_1 of block A in the copolymer itself is assumed to be 0.5.

Figure 6. The scattered intensity S(q) expected at high temperature ($T \to \infty$) is plotted against q, where the calculation is for the mixture containing various indicated volume fractions ϕ_h of polystyrene of M_w 35,000 added to a styrene-butadiene diblock copolymer of block molecular weights 16,850 and 5,150, respectively. The location q* of the intensity maximum on each curve is indicated by a dot. Note that q* gradually decreases toward zero as ϕ_h is increased.

Figure 7. Similar to Figure 6, but calculated for the addition of polystyrene of M_w 70,000 to the same styrene-butadiene diblock copolymer. Note that between $\phi_h = 0.25$ and 0.30, q* jumps discontinuously from a finite value to zero, indicating an abrupt changeover from a microphase separation behavior to a macrophase separation behavior as the volume of added polystyrene is increased.

Figure 8. The change in the peak scattering angle q* on addition of polystyrene of indicated molecular weight is calculated and is plotted against the weight fraction of the polystyrene in the mixture. The styrene-butadiene diblock copolymer is assumed to have block molecular weights of 16,850 and 5,150, respectively. With polystyrenes of M_w 70,000 and 100,000, the peak angle q* is seen to decrease discontinuously to zero as the fraction of the

homopolymer increases beyond certain values (abrupt changeover from a microphase separation to a macrophase separation behavior), whereas with polystyrene of lower molecular weights q* decreases continuously to zero (gradual merging of microphase separation and macrophase separation behaviors).

Figure 9. The spinodal temperatures for microphase separation (thick line) and for macrophase separation (thin line) are plotted against the weight fraction of polystyrene. The upper diagram is calculated for the mixture of styrene-butadiene copolymer (block molecular weights 16,850 and 5,150, respectively) with polystyrene of M_w 70,000, and the lower diagram for its mixture with polystyrene of M_w 35,000. The broken lines show the spinodal temperature which would have been realized if the microphase separation had not intervened. In these calculations, the values of the interaction energy density : given by equation (9) have been utilized.

Figure 10. The scattered intensity observed, at various temperatures indicated, with the mixture of the diblock copolymer with 50 weight percent polystyrene of M_w 2,200 is plotted against the scattering angle s (= $2\sin\theta/$). The ordinate $I(s)/$ ^{2} is the scattered intensity in absolute units (after correction for slit-smearing) divided by the square of the electron density difference between polystyrene and

polybutadiene at the temperature of measurement, and is equal to the structure factor S(q). The solid curves are calculated from the theoretical equations (1)-(8), with the ℓ values adjusted to give the best fit to the peak intensity.

Figure 11. The scattered intensity observed with the mixture containing 60 weight percent polystyrene of M_w 10,300.

Figure 12. The scattered intensity observed with the mixture containing 60 weight percent polystyrene of M_w 17,500.

Figure 13. The scattered intensity observed with the mixture containing 60 weight percent polystyrene of M_w 35,000.

Figure 14. The scattered intensity observed with the mixture containing 50 weight percent polystyrene of M_w 50,000.

Figure 15. The observed peak scattering angle s^* is plotted against the weight fraction of polystyrene for two series of mixtures, one containing polystyrene of M_w = 2,200 and the other M_w = 17,500. The solid lines give the values calculated on the basis of equations (2), (4)-(8).

Figure 16. The observed peak scattering angle s^* is plotted against the molecular weight of polystyrene for two series of mixtures, one containing 40 weight percent polystyrene and the other containing 60 weight

percent polystyrene. The solid lines give the values calculated from the theory.

Figure 17. The scattered intensity obtained with the mixture containing 60 percent polystyrene of M_w 2,200 is plotted in a manner suggested by the Ornstein-Zernike form of the structure factor, equation (13). The ordinate is equal to $\pm [I(s^*)/I(s) - 1]^{1/2}$, where the + sign is applicable for $q > q^*$ and the - sign for $q < q^*$. The slope of the straight line in the plot gives the correlation length ξ associated with the decay of short range order in the disordered phase.

Figure 18. The correlation length ξ, obtained with mixtures containing the indicated weight fraction polystyrene of M_w 2,200, is plotted against temperature. With the decrease in temperature, the correlation length increases and diverges at the spinodal temperature. The spinodal temperature is seen to decrease with increasing amounts of polystyrene in the mixture.

Figure 19. The plots illustrate the degree of fit achieved by the empirical equation (15) which assumes two independent components of scattering. The observed intensities were obtained with a mixture containing 70 weight percent polystyrene of M_w 17,500.

Figure 20. Plot of $1/\xi^2$ against $1/T$ for the mixture containing 40 weight percent polystyrene of M_w 10,300. The linear extrapolation of the high temperature data to $1/\xi^2 = 0$ gives the spinodal temperature T_s for

microphase separation, and the first deviation of the observed data from the straight line suggests the onset of microphase separation.

Figure 21. The plot of the reciprocal of observed peak intensity $I(s^*)/\Delta\rho^2$ against $1/T$, obtained with five mixtures containing various amounts of polystyrene of M_w 2,200, are superposed into a single curve by horizontal shifting. The slope of the common straight line drawn gives the value $A = 1.19$ cal/cm^3, when the interaction energy density Λ is expressed as $A+BT$. □ : 30 wt.% polystyrene; ▲ : 40 wt.%; △ : 50 wt.%; ■ : 60 wt.%; ○ : 70 wt.%.

Figure 22. Plots similar to those shown in Figure 21, but here for the mixtures containing 60 weight percent of polystyrene of ○ : M_w 2,200; ■ : M_w 4,000; △ : M_w 10,300; ▲ : M_w 17,500; and □ : M_w 35,000. For the latter three mixtures the peak intensity $I(s^*)$ were evaluated by fitting the scattered intensity curve to the empirical equation (15). The slope of the straight line again gives $A = 1.19$ cal/cm^3.

Figure 23. The spinodal temperature T_s for microphase separation, determined for mixtures containing polystyrene of M_w 2,200, is plotted against the weight fraction of polystyrene. ○ : T_s obtained from the plot of reciprocal peak intensity against $1/T$ and □ : T_s obtained from the plot of $1/\xi^2$ against $1/T$. The solid curve gives the T_s calculated from theory with use of the value of Λ given by equation (9).

Figure 24. The spinodal temperature T_s, obtained for mixtures containing 60 percent polystyrenes, is plotted against the molecular weight of polystyrene. o : obtained from $1/I(s^*)$ vs. $1/T$; □ : obtained from $1/\xi^2$ vs. $1/T$. The solid curve gives the values calculated from theory with the use of the χ values given by equation (9).

Figure 25. Plotted against temperature are the χ values evaluated on the basis of equation (17) from the observed peak intensity $I(s^*)$. The broken straight line drawn represents the average of all points and can be represented by $\chi = 1.19 - 5.0\times10^{-4}T$ (cal/cm^3). The solid straight line represents χ values given by equation (9) which was previously determined from the observed cloud points. □ : mixture containing 30% polystyrene of M_w 2,200; ● : 40% M_w 2,200; o : 50% M_w 2,200; ▲ : 60% M_w 2,200; ▽ : 70% M_w 2,200; ■ : 60% M_w 4,000; ▽ : 40% M_w 10,300; ▼ : 60% M_w 10,300; ◇ : 60% M_w 17,500; ◆ : 70% M_w 17,500.

Figure 26. Plotted against temperature are χ values evaluated on the basis of equation (19) from the χ values. For the symbols, see Figure 25.

Figure 27. Schematic rendering of phase diagrams expected for the mixtures of styrene-butadiene block copolymer with polystyrene. Diagrams a, b and c represent cases with successively lower molecular weight polystyrene.

Table I

Composition of Mixtures Studied

M_w of PS \ wt. fraction of PS	0.30	0.40	0.50	0.60	0.70
2,200	clear	clear	clear	clear	clear
4,000				clear	
10,300		clear		clear	
17,500		clear		clear	clear
35,000				clear	
50,000			clear		
100,000	turbid		turbid		

Table IIa

Spinodal Temperature T_s Evaluated from $1/I(s^*)$ vs. $1/T$

M_w of PS	Wt. fraction of polystyrene 0.30	0.40	0.50	0.60	0.70
2,200	125°C	107	78	53	14
4,000				68	
10,300		167 (?)[b]		133[a]	
17,500		205[a](?)[b]		176[a](?)[b]	160[a](?)[b]
35,000				210[a](?)[b]	

Note: a) $I(s^*)$ was evaluated through fit to the empirical equation (15).

b) These values are less reliable than others.

Table IIb

Spinodal Temperature T_s Evaluated from $1/\xi^2$ vs. $1/T$

M_w of PS	Wt. fraction of polystyrene				
	0.30	0.40	0.50	0.60	0.70
2,200	105°C	89	70	52	32
4,000				79	
10,300		147		139[a]	
17,500					132[a]

Note: a) ξ was evaluated through fit to the empirical equation (15).

FIGURE 1

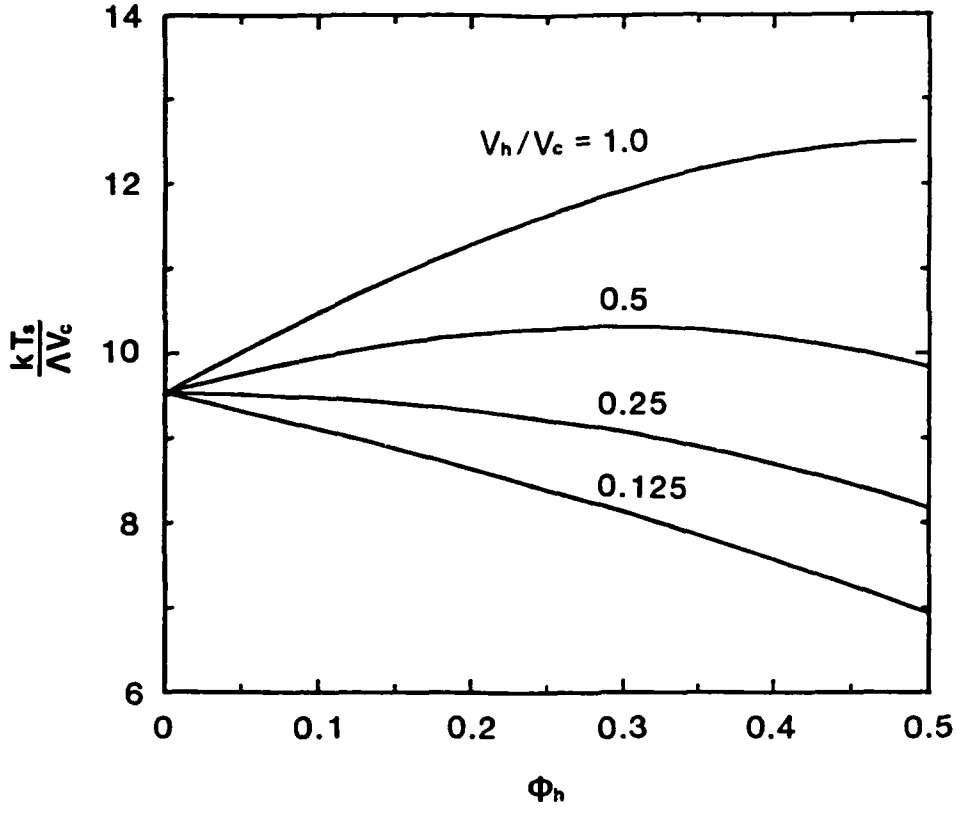

FIGURE 2

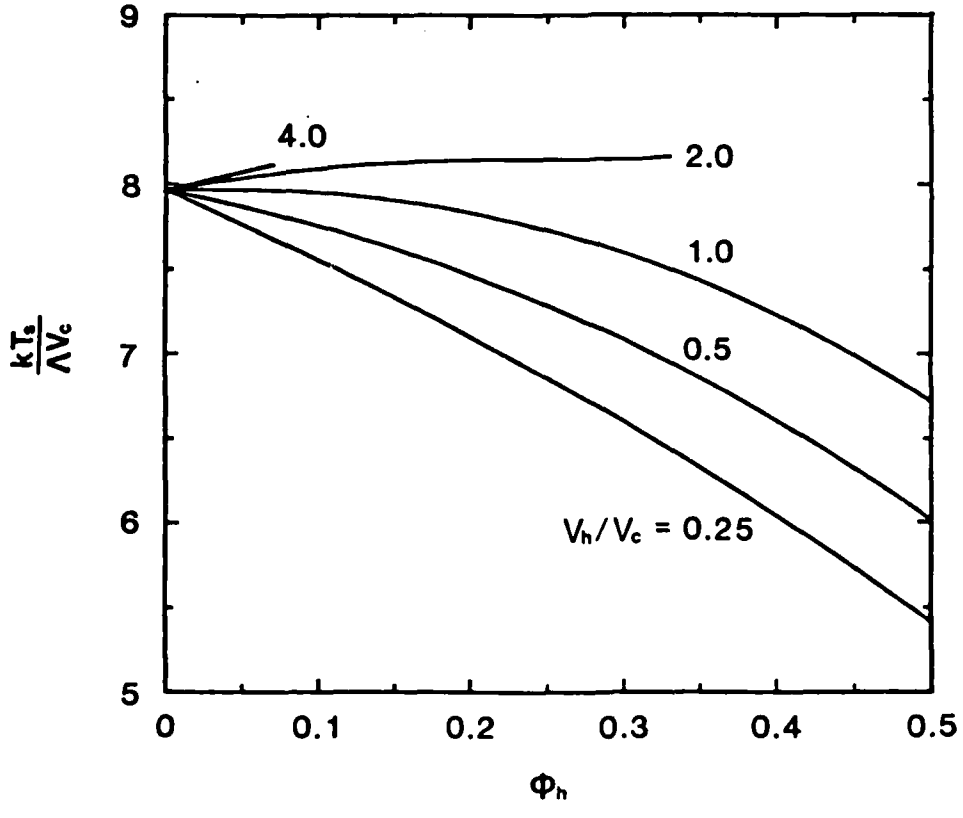

FIGURE 3

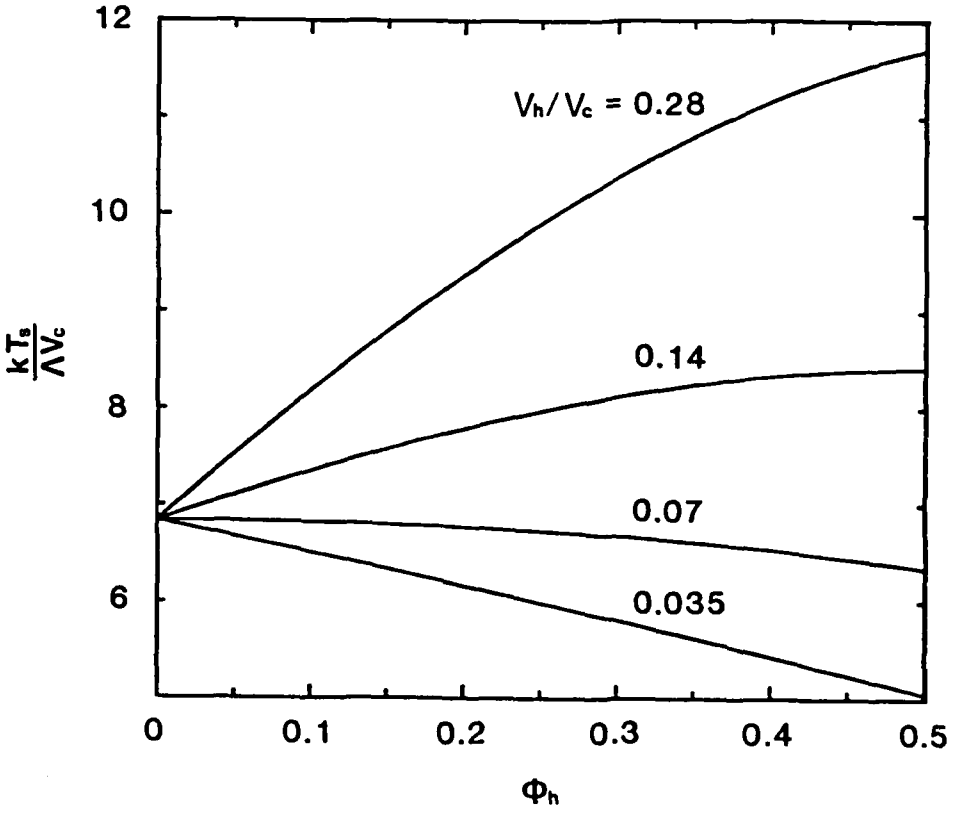

FIGURE 4

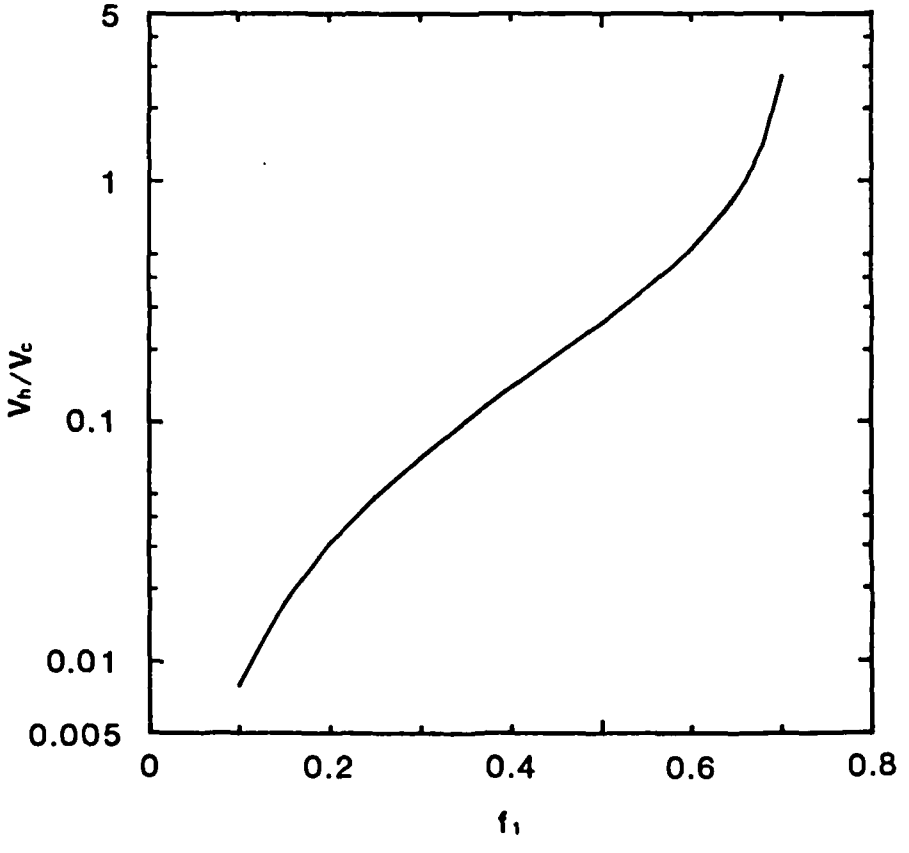

FIGURE 5

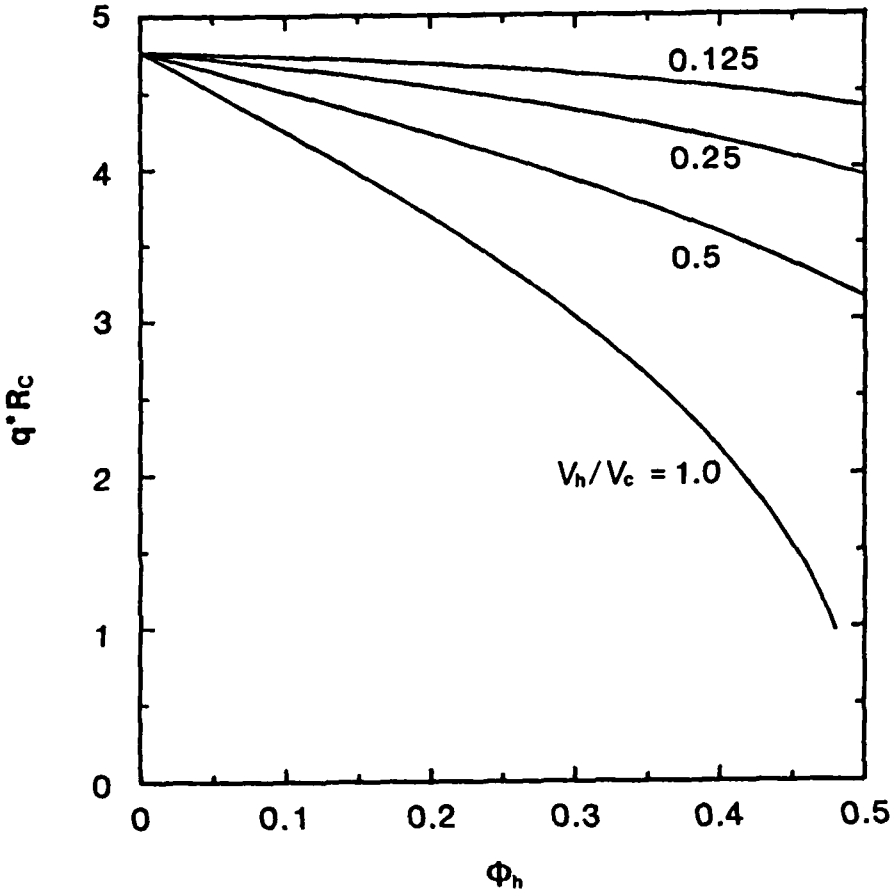

FIGURE 6

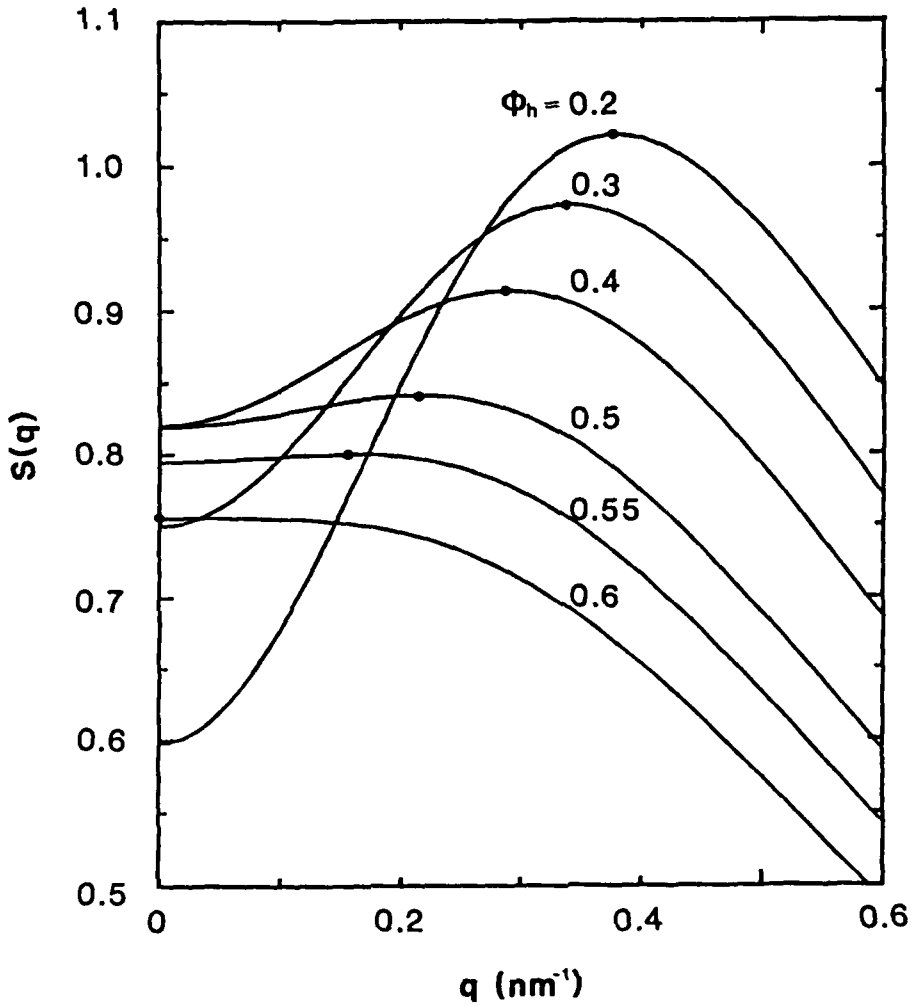

FIGURE 7

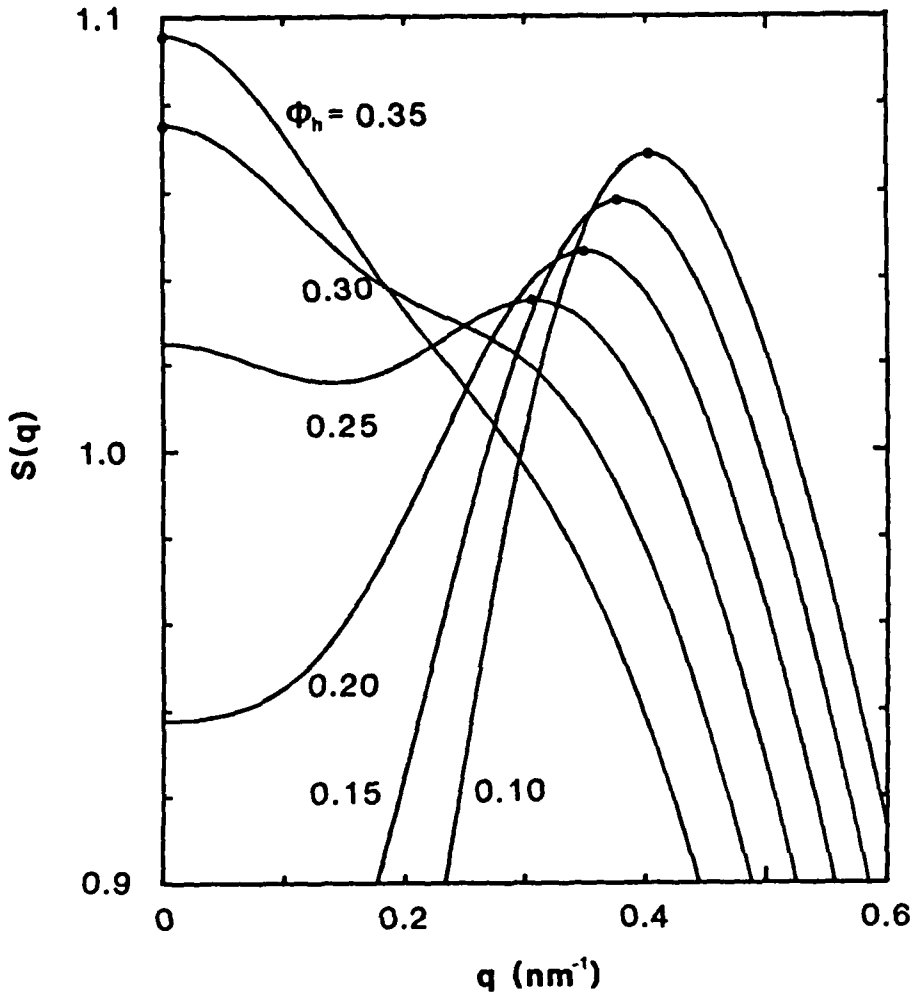

FIGURE 8

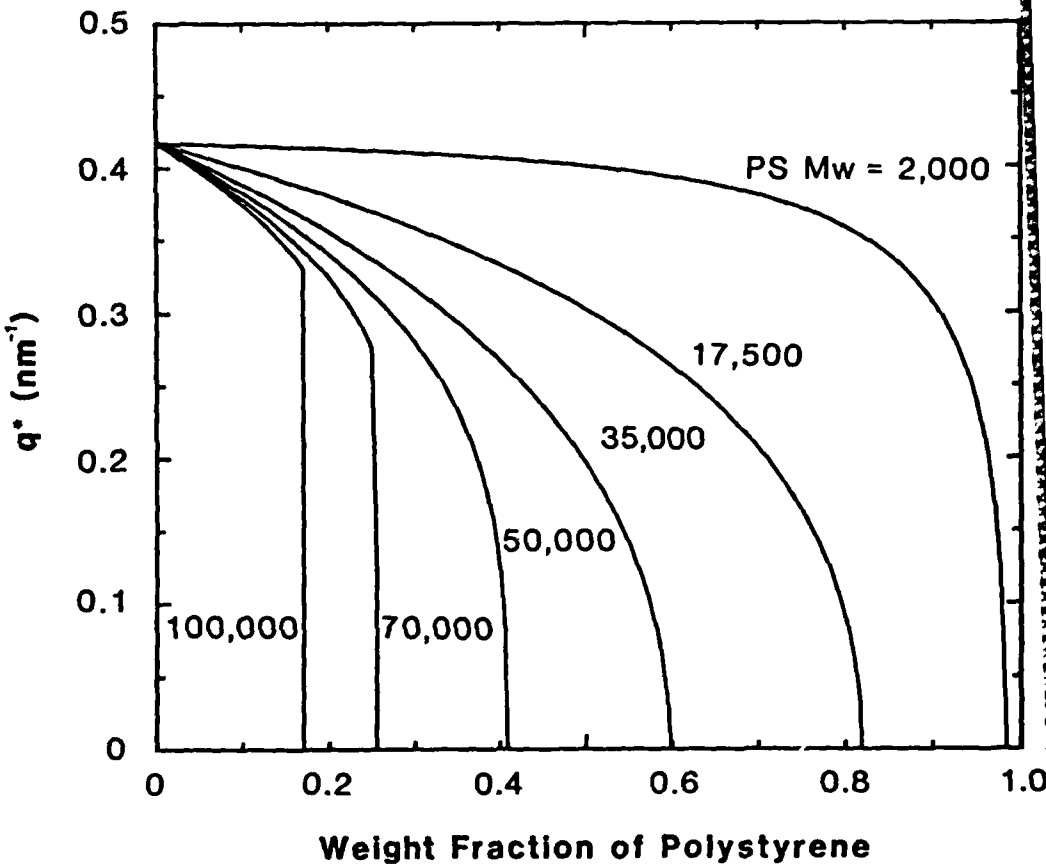

FIGURE 9

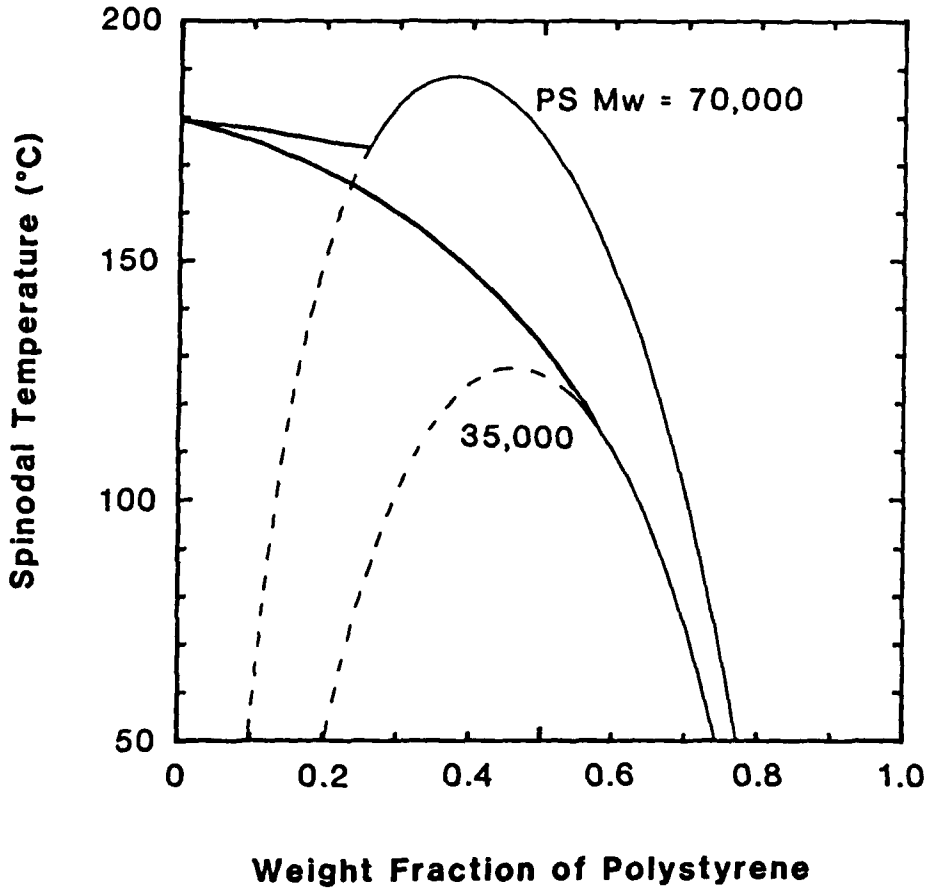

FIGURE 10

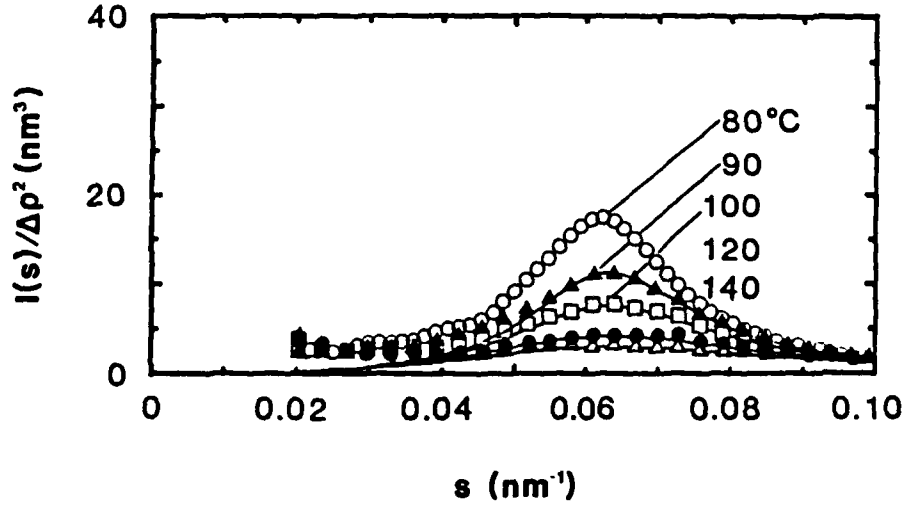

FIGURE 11

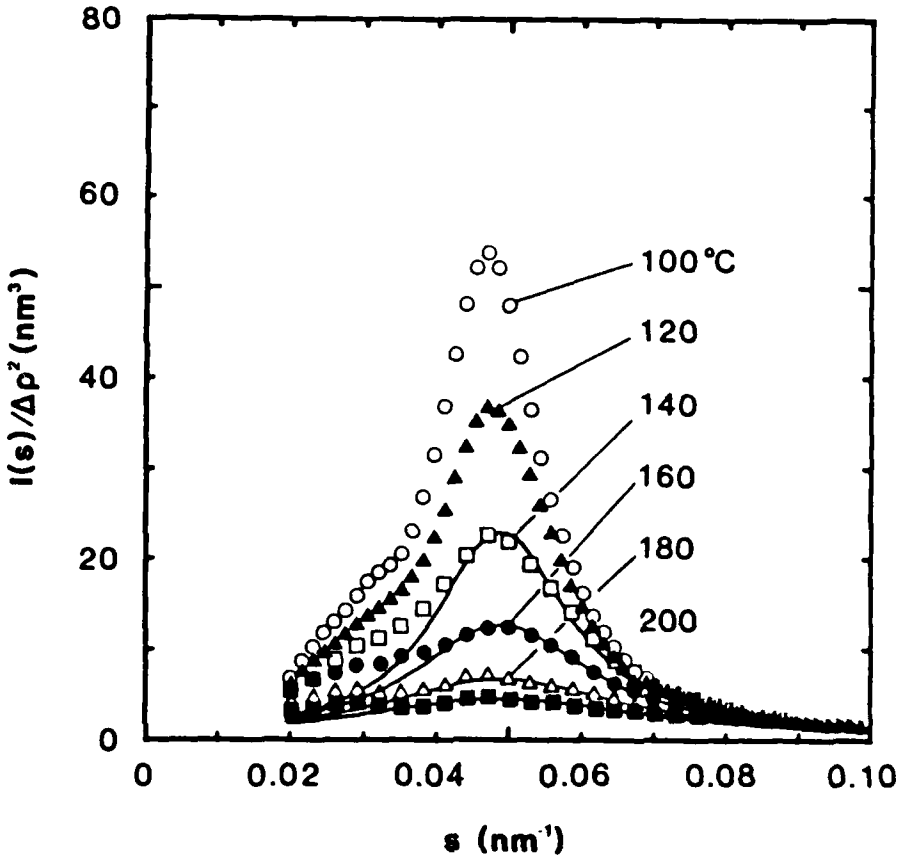

FIGURE 12

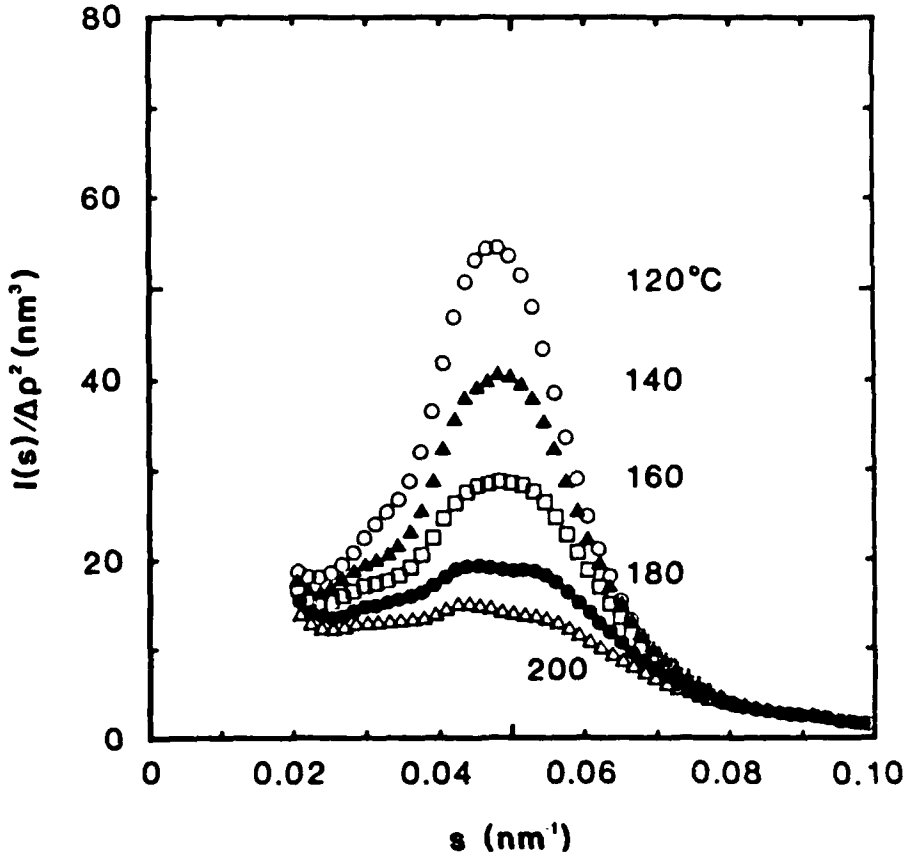

FIGURE 13

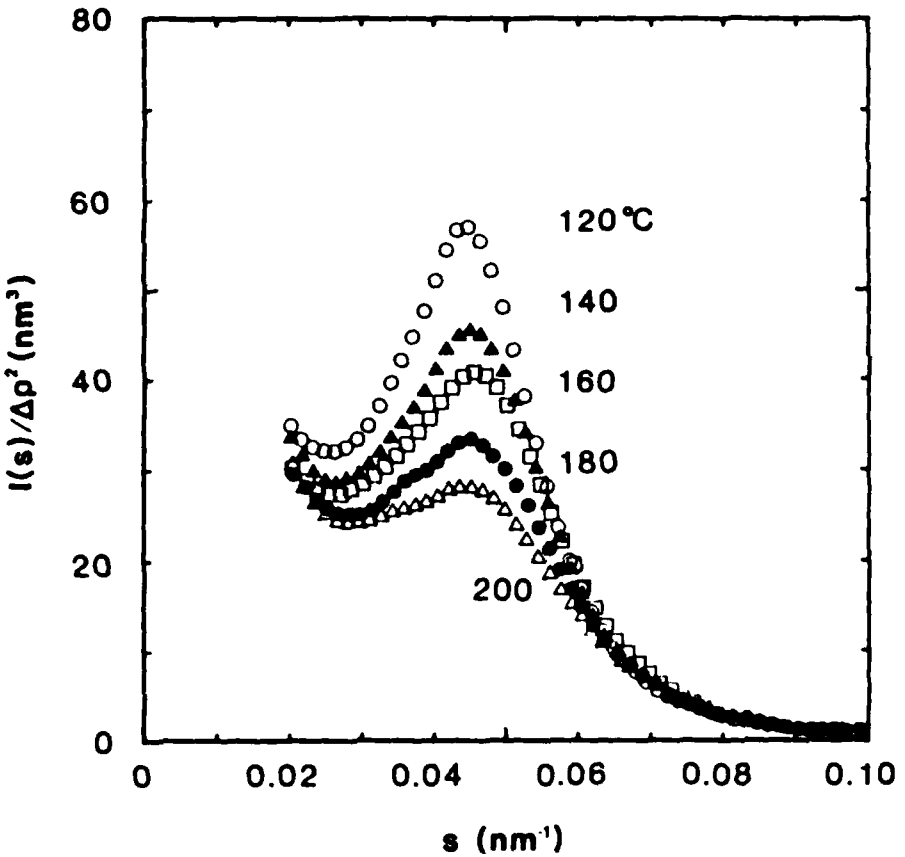

FIGURE 14

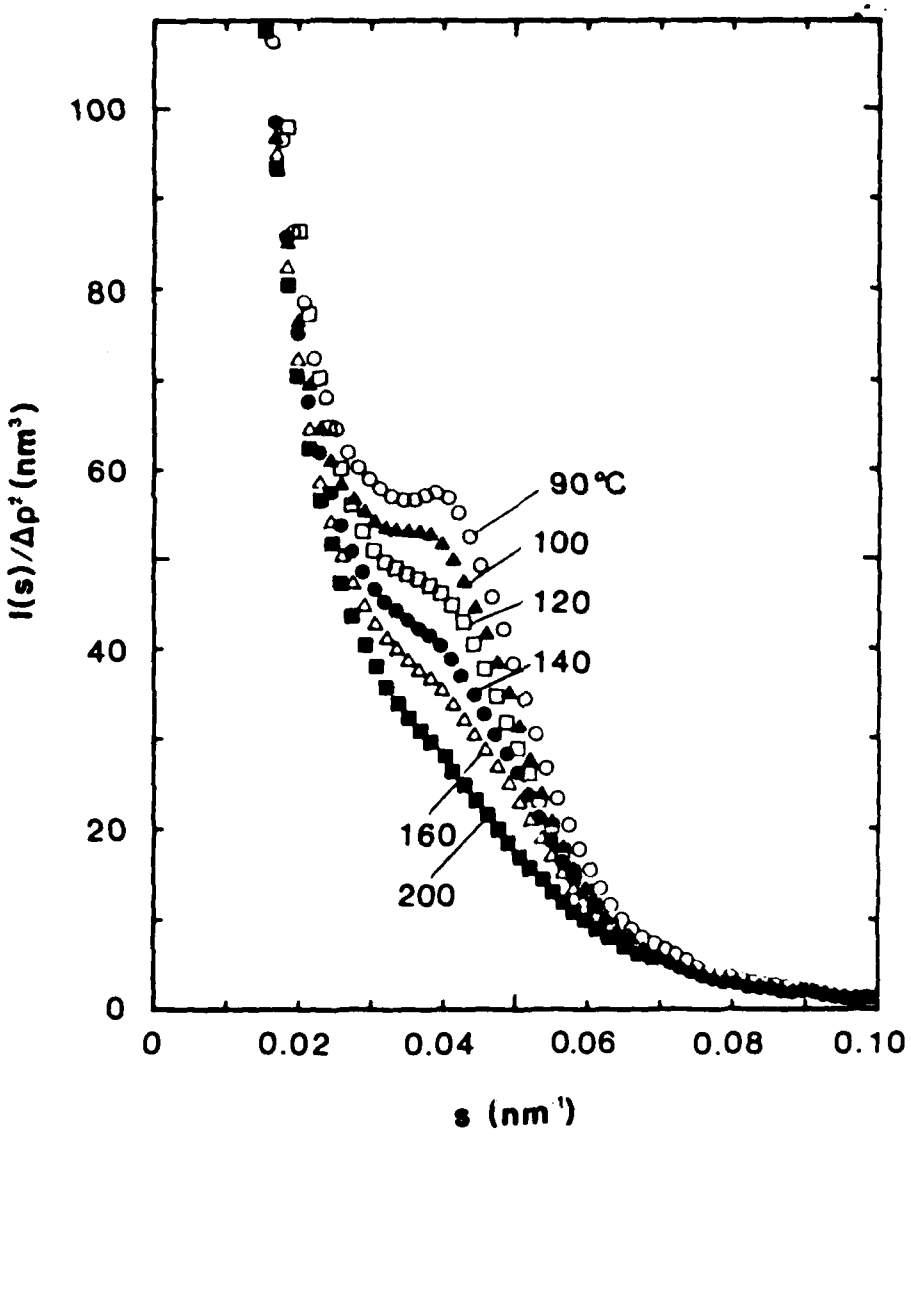

FIGURE 15

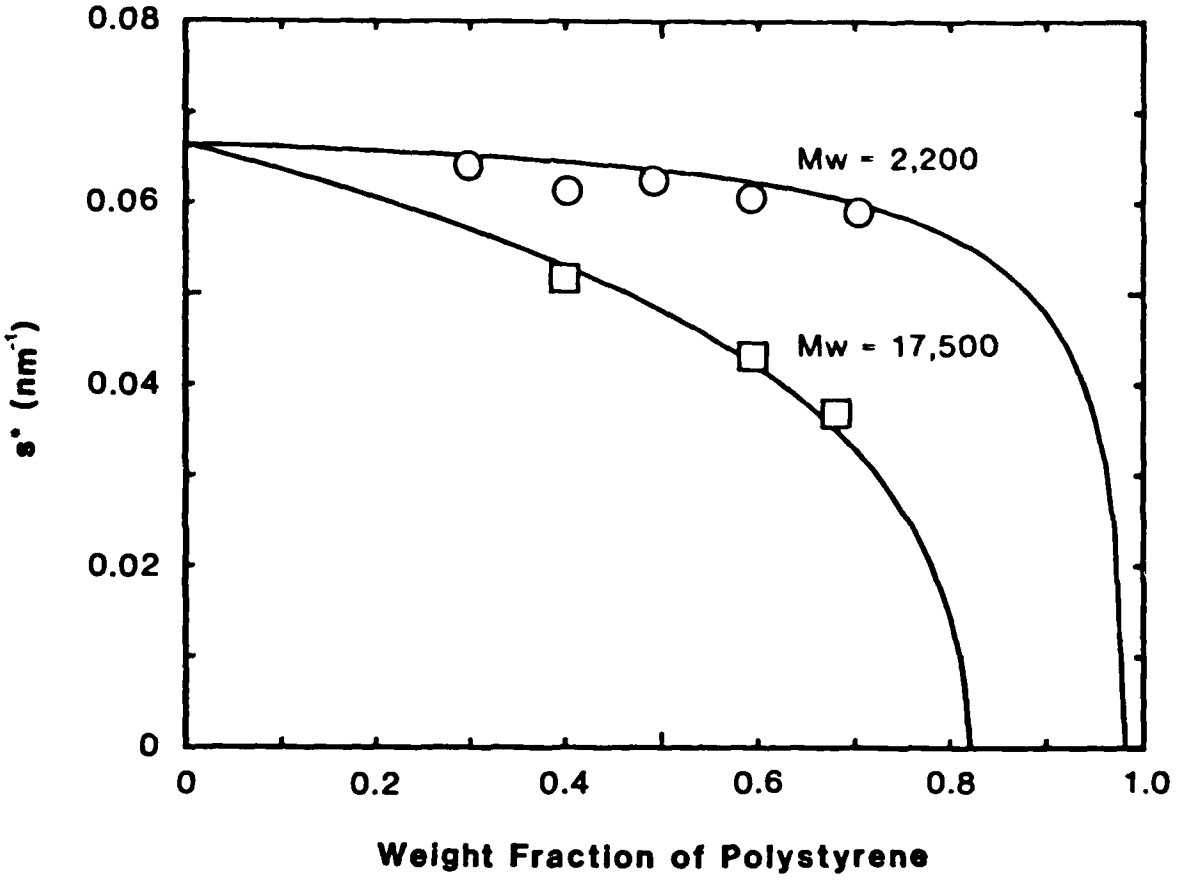

FIGURE 16

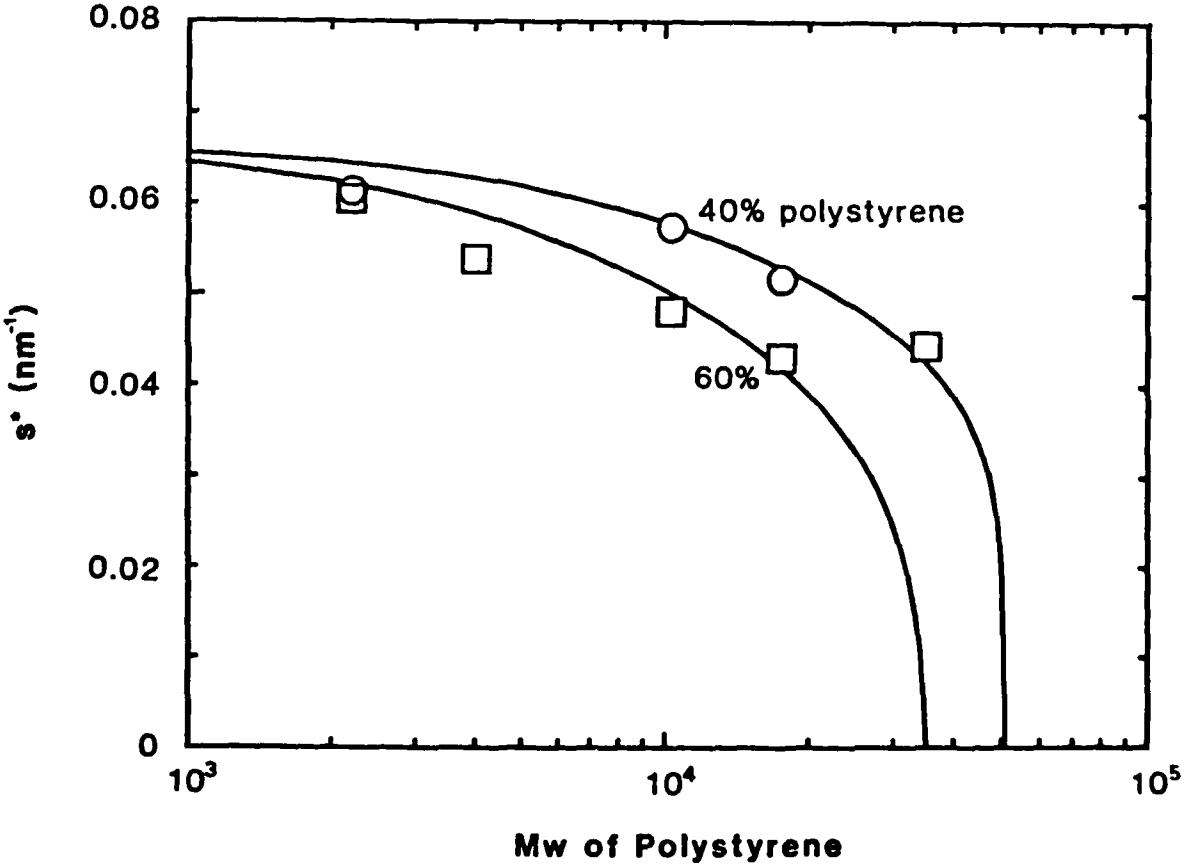

FIGURE 17

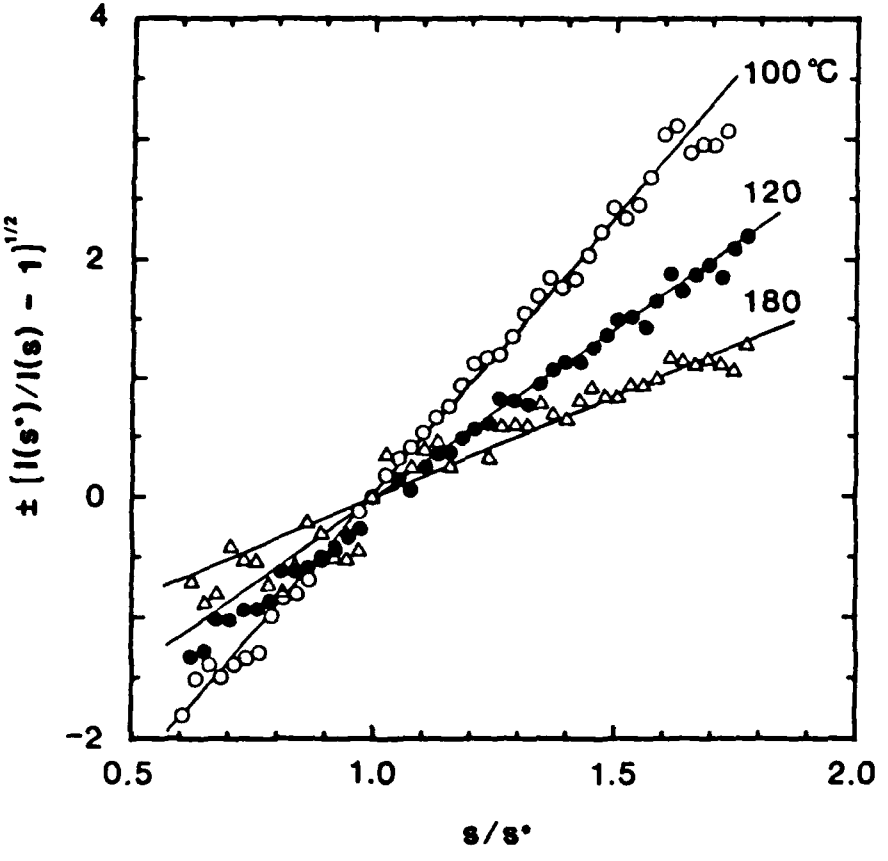

FIGURE 18

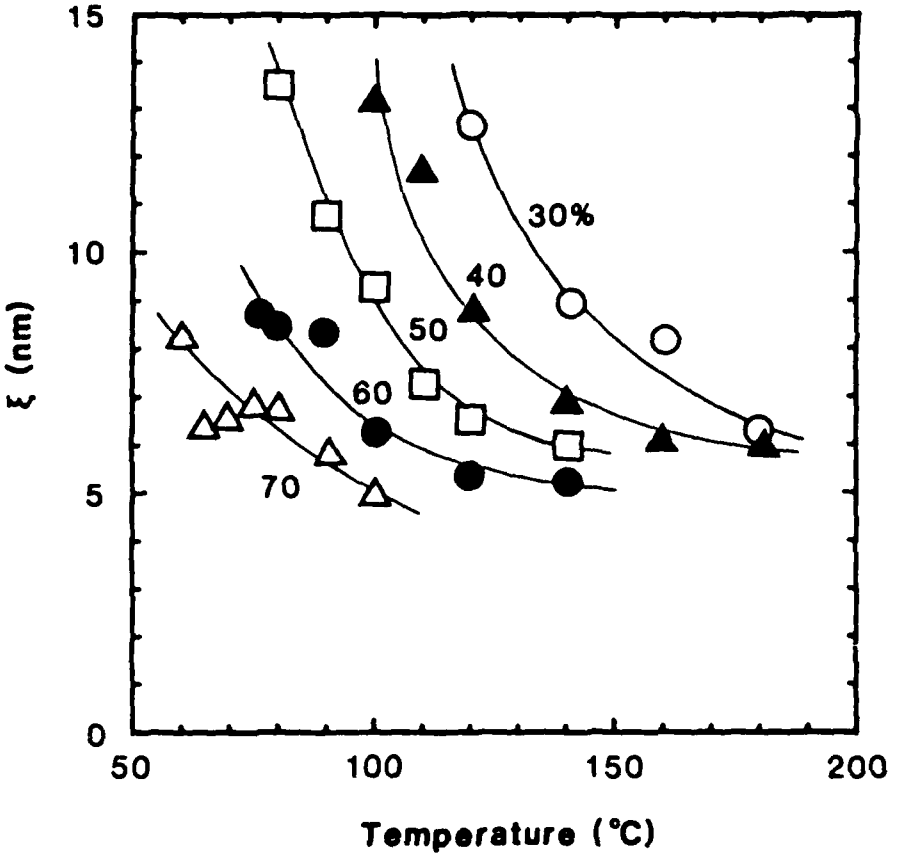

FIGURE 19

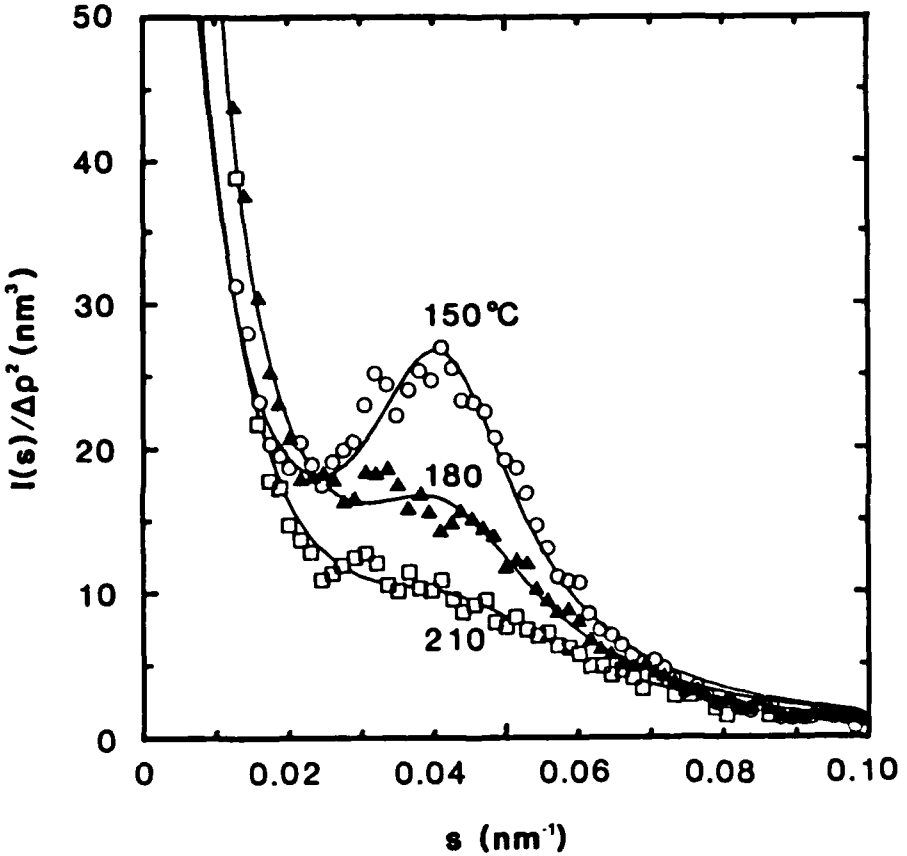

FIGURE 20

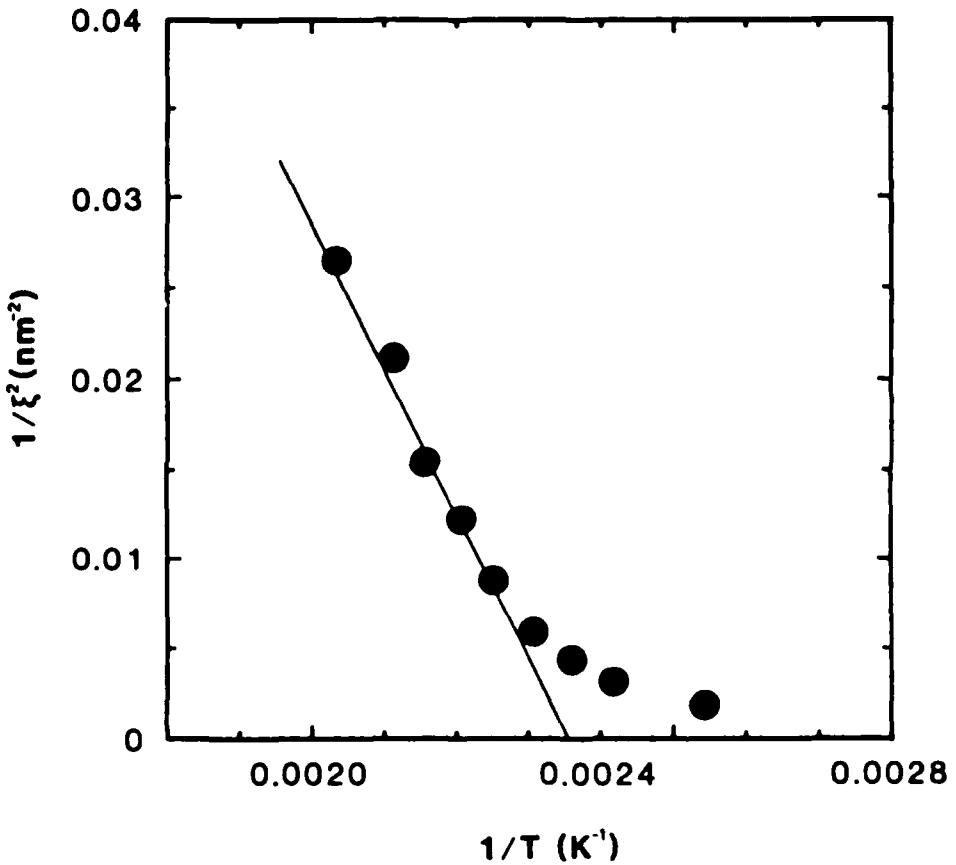

FIGURE 21

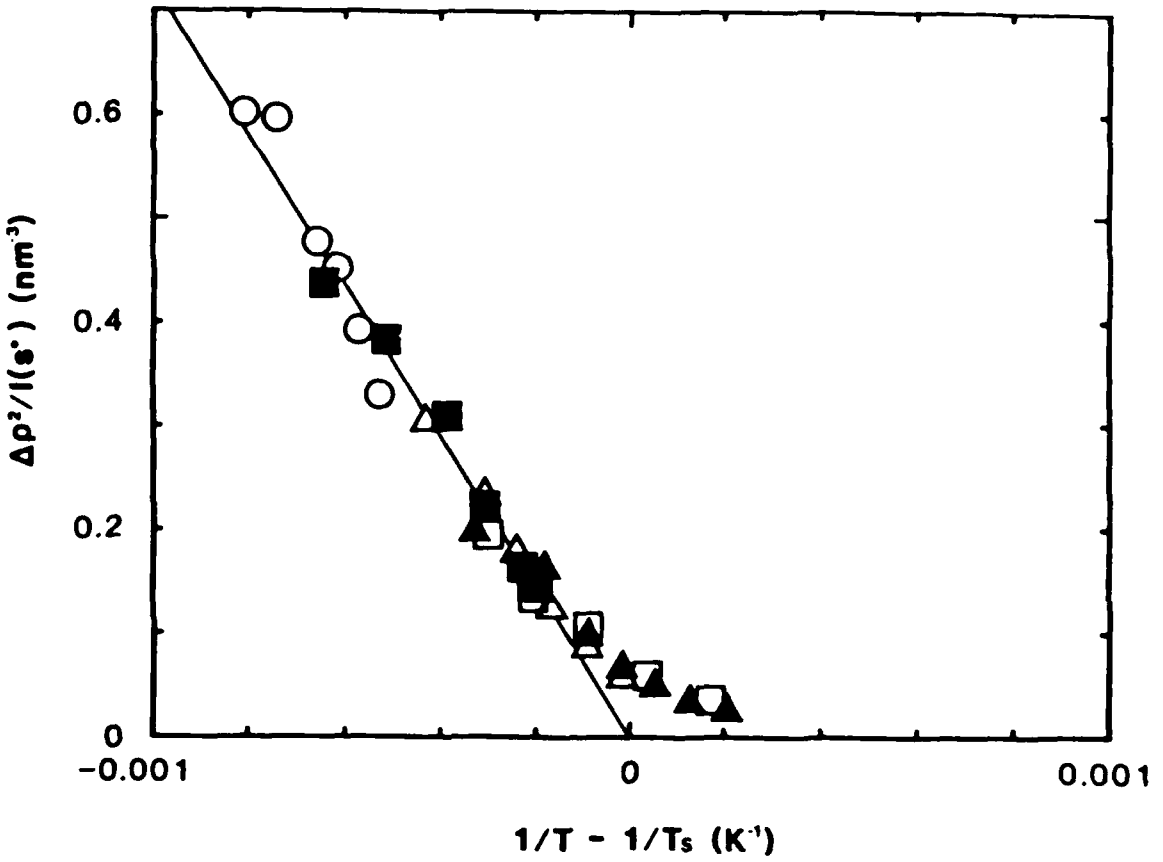

FIGURE 22

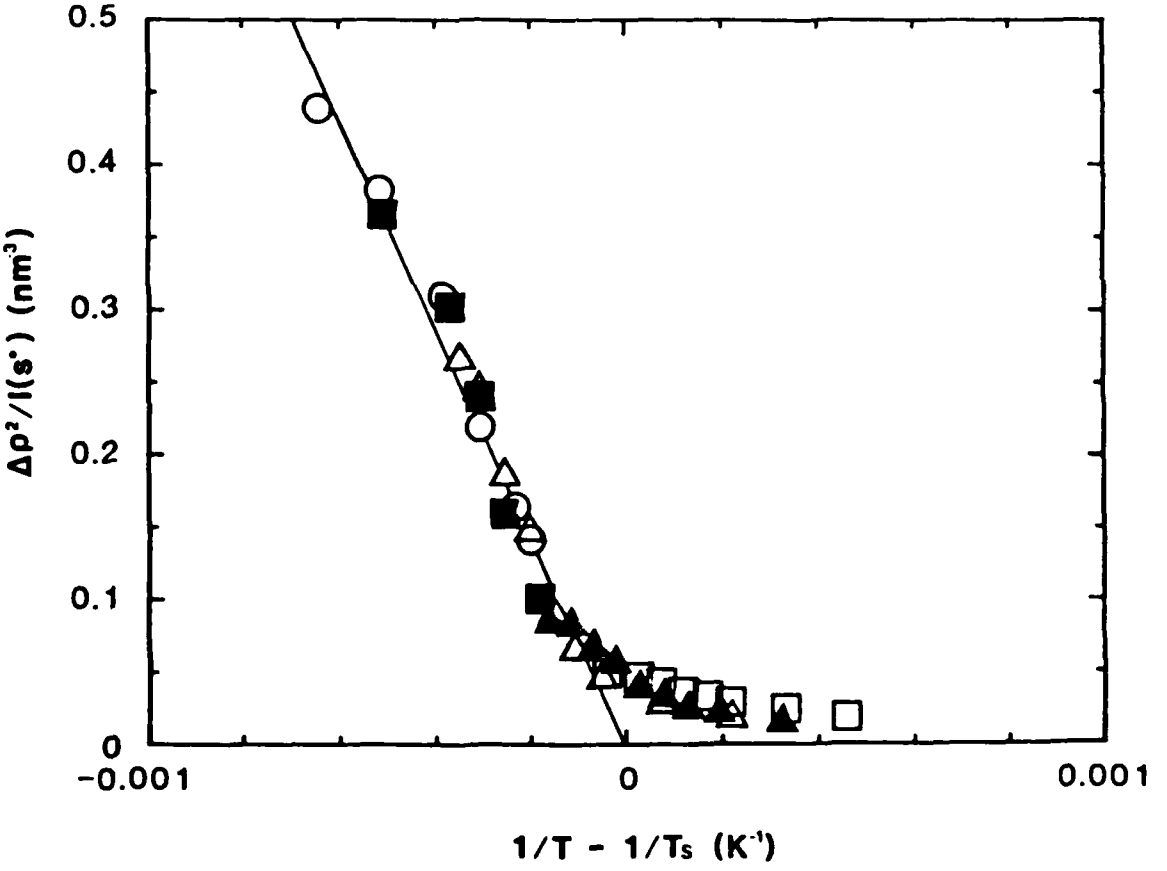

FIGURE 23

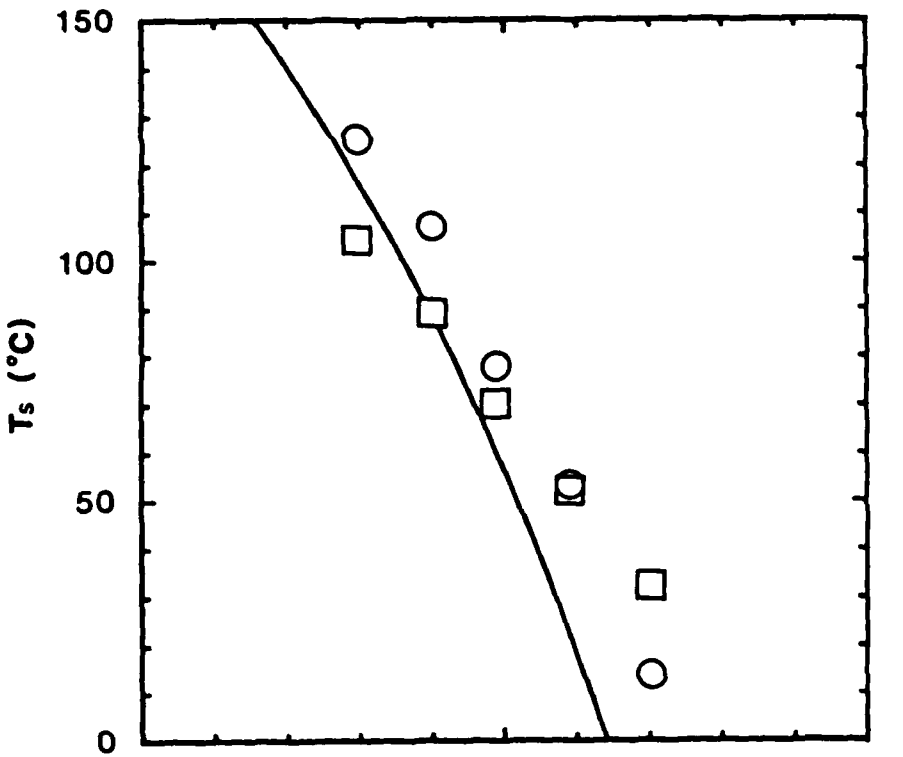

FIGURE 24

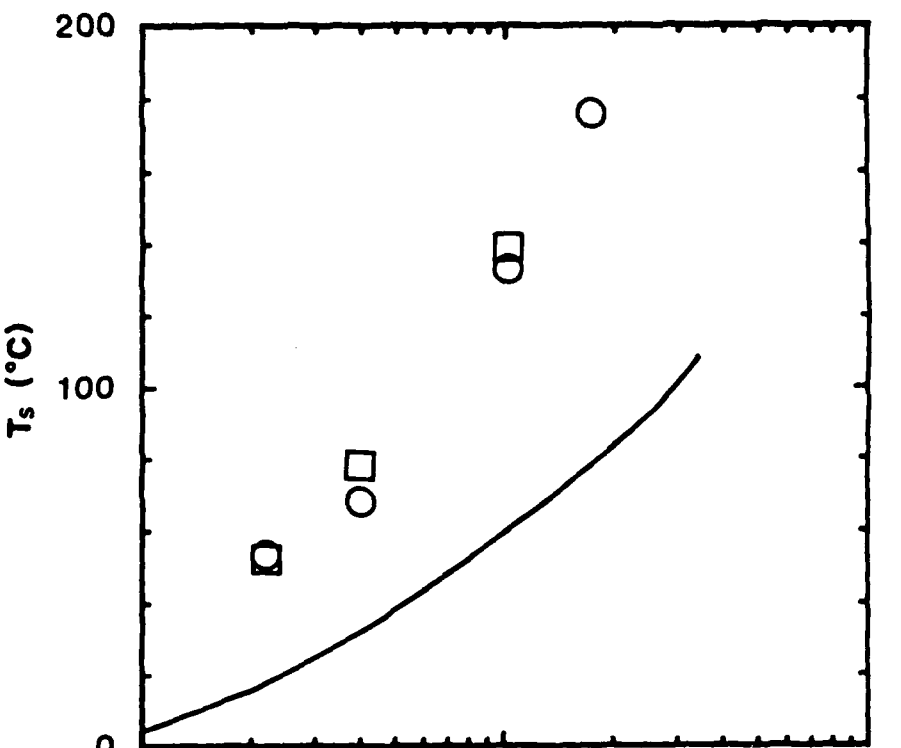

FIGURE 25

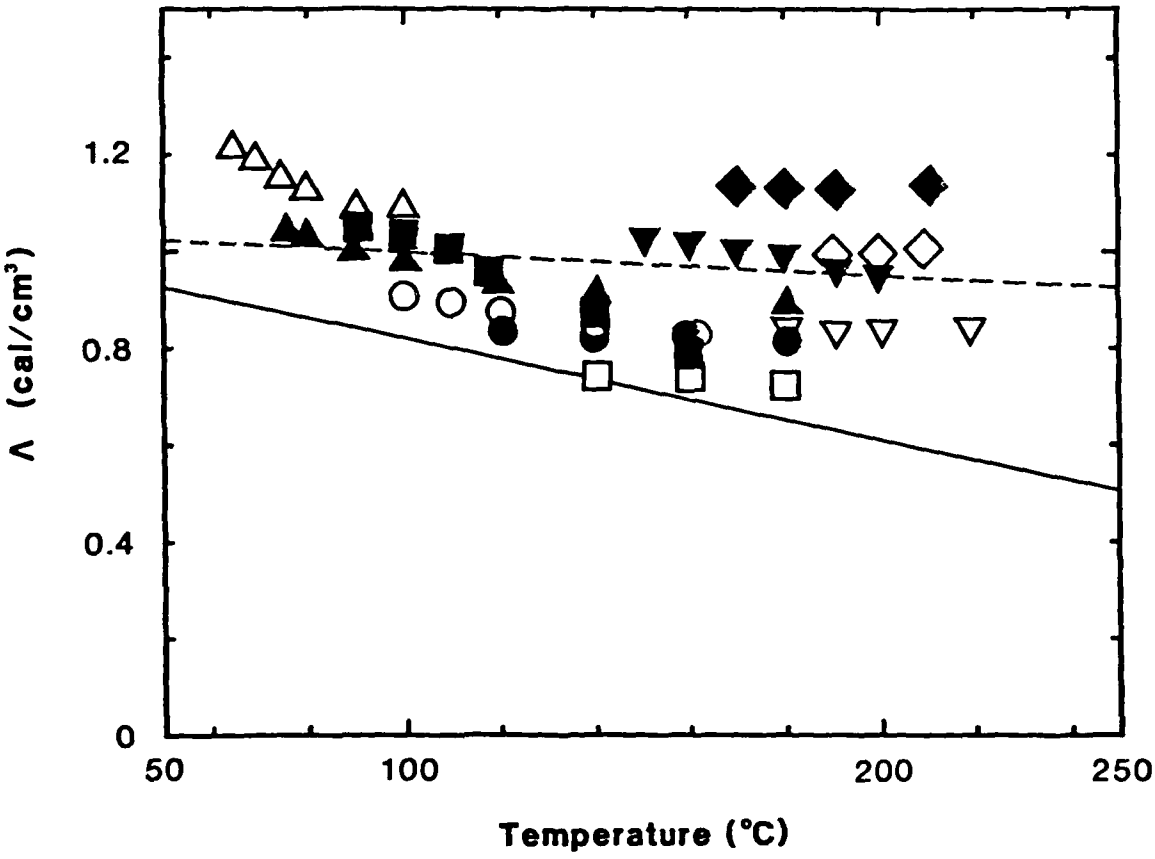

FIGURE 26

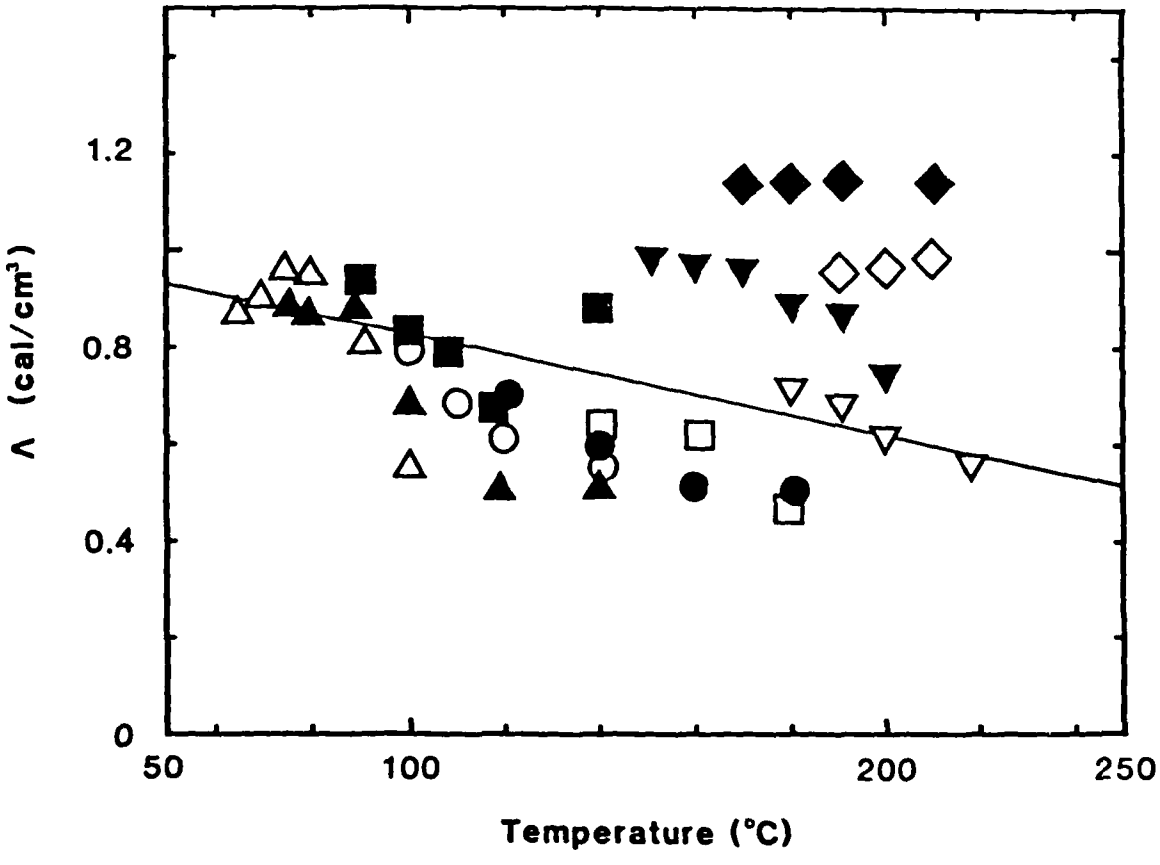

FIGURE 27A

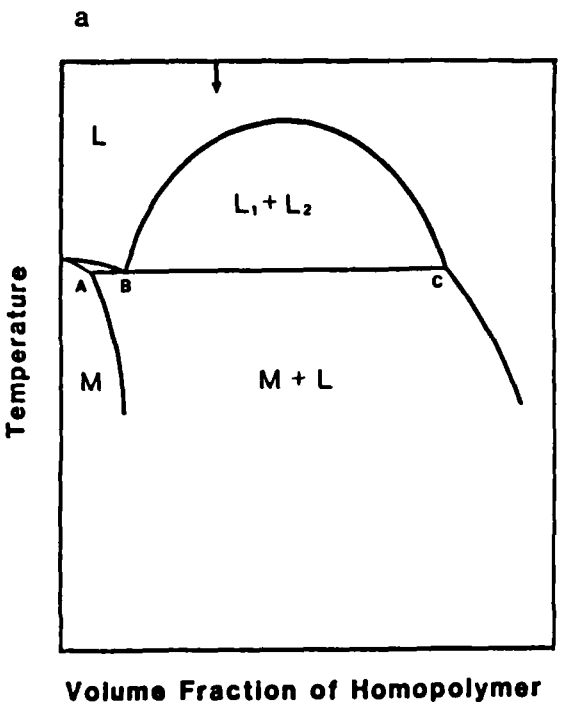

FIGURE 27B

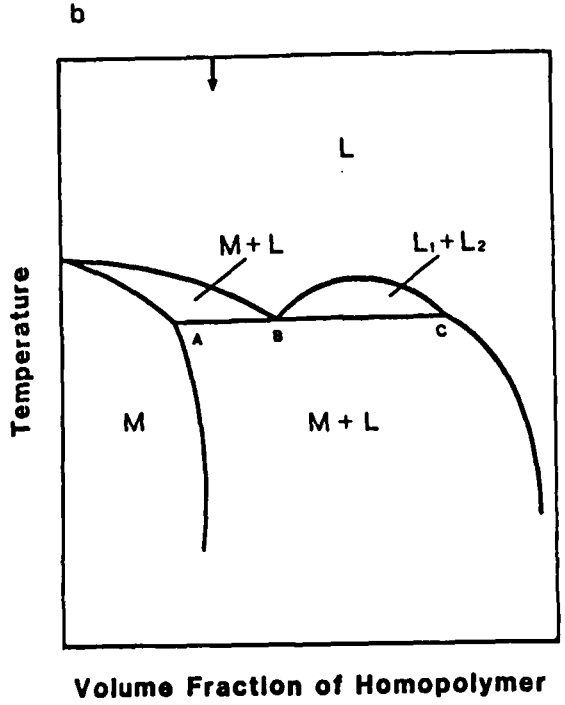

FIGURE 27C

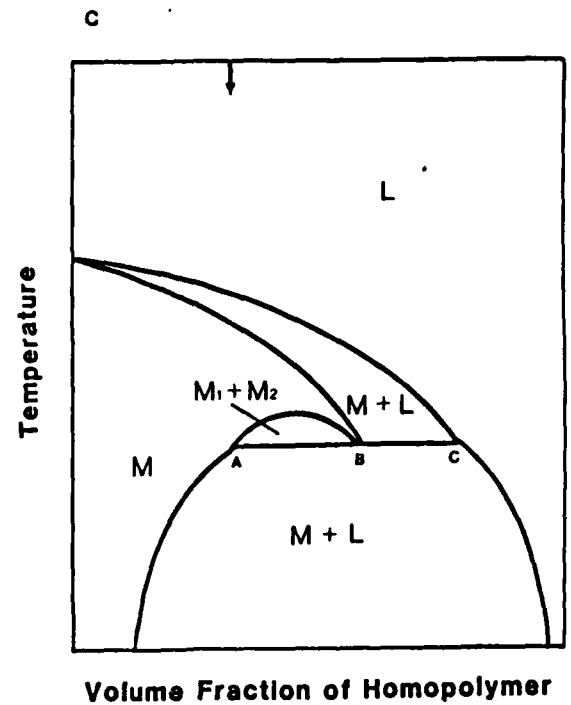

DL/1113/86/2

TECHNICAL REPORT DISTRIBUTION LIST, GEN

	No. Copies
Office of Naval Research Attn: Code 1113 800 N. Quincy Street Arlington, Virginia 22217-5000	2
Dr. Bernard Douda Naval Weapons Support Center Code 50C Crane, Indiana 47522-5050	1
Naval Civil Engineering Laboratory Attn: Dr. R. W. Drisko, Code L52 Port Hueneme, California 93401	1
Defense Technical Information Center Building 5, Cameron Station Alexandria, Virginia 22314	12 high quality
DTNSRDC Attn: Dr. H. Singerman Applied Chemistry Division Annapolis, Maryland 21401	1
Dr. William Tolles Superintendent Chemistry Division, Code 6100 Naval Research Laboratory Washington, D.C. 20375-5000	1
Dr. David Young Code 334 NORDA NSTL, Mississippi 39529	1
Naval Weapons Center Attn: Dr. Ron Atkins Chemistry Division China Lake, California 93555	1
Scientific Advisor Commandant of the Marine Corps Code RD-1 Washington, D.C. 20380	1
U.S. Army Research Office Attn: CRD-AA-IP P.O. Box 12211 Research Triangle Park, NC 27709	1
Mr. John Boyle Materials Branch Naval Ship Engineering Center Philadelphia, Pennsylvania 19112	1
Naval Ocean Systems Center Attn: Dr. S. Yamamoto Marine Sciences Division San Diego, California 91232	1

END

8-87

DTIC